R441

File Copy

TRACK TRAIN DYNAMICS
TECHNICAL DOCUMENTATION

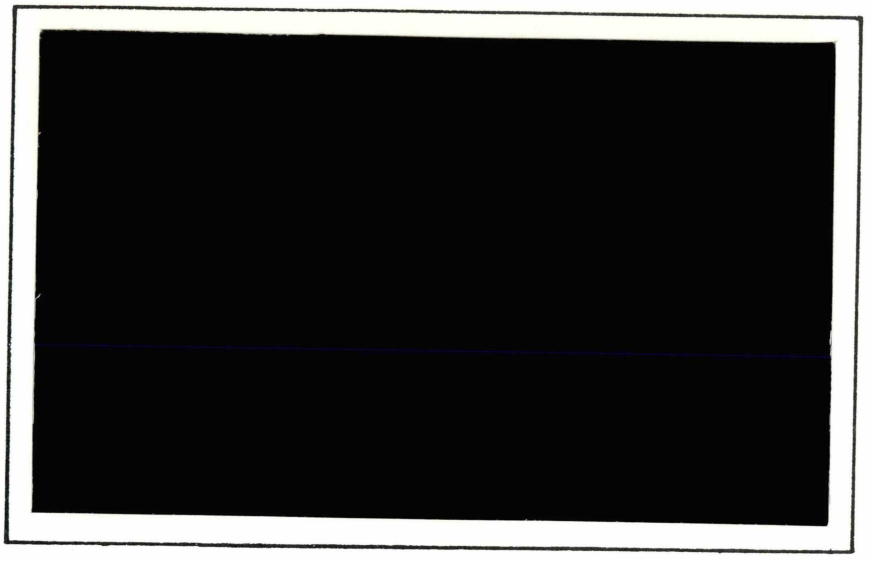

TRACK TRAIN DYNAMICS
AAR

ERNATIONAL GOVERNMENT-INDUSTRY RESEARCH PROGRAM ON TRACK-TRAIN DYNAMICS

Association of American Railroads

Research and Test Department

DYNAMIC ANALYSIS OF A VEHICLE/BRIDGE SYSTEM FOR CALCULATION OF IMPACT LOADS

REPORT NO. R-447

Satya P. Singh

Som P. Singh

V. K. Garg

December, 1981

AAR Technical Center

Chicago, Illinois

1. REPORT NO.	2. REPORT DATE	3. PERIOD COVERED
R-447	December, 1981	

4. TITLE AND SUBTITLE

Dynamic Analysis of a Vehicle/Bridge System for Calculation of Impact Loads

5. AUTHOR(S)

Satya P. Singh, Som P. Singh and V. K. Garg

6. PERFORMING ORGANIZATION NAME AND ADDRESS

Association of American Railroads
Track-Train Dynamics, Phase III
3140 South Federal Street
Chicago, Illinois 60616

7. TYPE OF REPORT

Analytical

8. CONTRACT OR GRANT NO.

DOT FR 64228

9. SPONSORING AGENCY NAME AND ADDRESS

Federal Railroad Administration
Department of Transportation
400 Seventh Street, S.W.
Washington, D.C. 20590

10. NO. OF PAGES

61

11. NO. OF REFERENCES

9

12. SUPPLEMENTARY NOTES

13. ABSTRACT

A mathematical model to obtain various generalized physical properties, such as mass, stiffness, damping and loads, has been derived to evaluate the dynamic response of a coupled vehicle(s)/bridge system. The analytical results, in terms of inertial-load and deflection increments, were interpreted as impact factors for member stresses and node deflections, respectively. AREA Specifications for impact loads and actual field test results on two truss bridges were used to compare the model results.

This study was undertaken to demonstrate only the applicability of such an analysis in impact evaluation. The basic objective was, within practical limitations, to develop a simple mathematical model for impact analyses, in order to better understand the mechanism involved. This study is only preliminary, and is not intended to replace existing AREA Specifications for impact loads.

14. SUBJECT TERMS

Bridge Design
Bridge Impact
Bridge Stresses
Vehicle/Bridge Interaction

15. AVAILABILITY STATEMENT

J. G. Britton, Executive Director
Association of American Railroads
Technical Center
3140 South Federal Street
Chicago, Illinois 60616

EXECUTIVE SUMMARY

An analytical method of obtaining a dynamic structural analysis of a coupled bridge-vehicle(s) system is presented to selectively demonstrate the application of a mathematical model to actual train-bridge interactions, using two specific truss bridges.

A judicious adaptation of a sophisticated method of analysis, such as the one used here which uses simplifying assumptions, requires a comparison of its theoretical results with those obtained by running tests on congruent systems. A comparison with specific test results was, therefore, made to evaluate the present analysis. Even if this comparison does not depict actual bridge component behaviors, it could at least be expected to provide information on the range of such parameters.

The analytical results were also compared with the current AREA Specifications for impact loads. The model can be used to determine the dynamic amplifications of stresses in individual or critical members in bridges and to provide information on dynamic augments, so that the minimum structural requirements, consistent with the resulting impact effects, could be determined, in order to provide economical and safe designs for bridge systems.

TABLE OF CONTENTS

TABLE OF CONTENTS (CONTINUED)

TABLE OF CONTENTS (CONTINUED)

LIST OF TABLES

LIST OF FIGURES

LIST OF FIGURES (CONTINUED)

1.0 INTRODUCTION

The generation of inertial reactions between a railroad bridge and moving vehicles is of great significance. The rather popular terminology used for this inertial reaction is impact factor, and is defined as the ratio of the maximum dynamic response to the maximum static response, minus one.

The subject of impact has been studied for over a century. In the past, major efforts in this direction, under the auspices of various organizations, such as the AREA, AAR, etc., had been to secure factual data on the dynamic effects of moving loads on bridges, based on experimental investigations of the bridges under high speed trains. The AREA Design Specifications [3]* for impact loads on railroad bridges were developed on the basis of the results from these extensive field tests.

An attempt to develop analytical studies of impact phenomena was started by Willis [6]. This was later supplemented with significant contributions by Timoshenko [7] in the 1920's, and by Inglis [8] in the 1930's. However, all of these studies considered either a single smooth-running mass, a single moving pulsating force, or a single axle, consisting of both a sprung and an unsprung mass with a dashpot. These approaches fell short of being realistic interaction idealizations, and subsequent efforts in this direction were lacking, until a thesis was written by Dhar [1].

The impact formula, as presently used, is empirical and was obtained by means of a statistical analysis of the earlier test results; therefore, to uniformly augment a static load solution with these empirical dynamic load factors is certainly not conservative, if these factors have been underestimated, nor economical if they have been overestimated. Also, a basic understanding of the actual impact mechanism and its correlation with the various design parameters of railway vehicles and bridges is lacking.

* The numbers in square brackets [ ] refer to the References, listed in Section 7.0 of this report.

To satisfy this need for an analytical solution, the present mathematical approach was sought and forms the basis for the present study.

The approach consisted of using the standard stiffness method to model the bridge structure as a lumped-mass system, having both vertical and longitudinal degrees-of-freedom. Each vehicle was realistically represented as either a four-axle or six-axle sprung/unsprung load system, having three degrees-of-freedom: bounce, roll, and pitch assigned to the sprung mass. Only the vehicle in its normal operating condition was considered, and the effects of vehicle truck hunting or braking, resulting in lateral or longitudinal motions of the bridge, were neglected. The resulting equations of motion for the vehicle-bridge system, to include the vehicle-bridge interactions, were then developed and solved to generate the dynamic impact factors for the member forces and nodal deflections.

It suffices to point out that the vibrational effects, resulting from the rolling motions of the locomotives and cars, are only one of the sources of impact forces in bridges, and that it would still be necessary to conduct field tests for the following purposes: (1) to complement and verify the analytical approach, and (2) to further determine the effects resulting from irregular track geometry, battered rail joints, out-of-round wheels and flat spots.

2.0 BRIDGE AND VEHICLE MODELS, AND THEIR EQUATIONS OF MOTION

2.1 Bridge Model

The bridge was considered to be composed of two planar structures: two trusses or two girders, interconnected by a simply supported rigid floor system; floor beams and stringers, and a bracing system. Each truss or girder was idealized as a lumped-mass model, consisting of planar assemblages of truss and beam elements, respectively. The in-plane displacements at the ends of each beam element were assumed to be rotations and normal translations, and those at the ends of each truss element were assumed to be axial deformations. One-half of the mass of each member was contributed to the joint with which it was connected. The mass of the floor system, which was composed of cross-beams, stringers and the track, was distributed, assuming simply supported reactions to the corresponding loaded joints in the bridge model. A simply supported rigid floor system implied that the total floor mass was uniformly distributed among the various loaded joints.

2.2 Vehicle Model

Each railway vehicle was idealized as a three degrees-of freedom model, consisting of a sprung rigid-body connected to either four or six wheel-axle sets. The carbody and trucks constituted the sprung mass, and the wheel-axle sets the unsprung mass of the system. The three degrees-of-freedom: bounce, pitch and roll assigned to the sprung mass were found to be sufficient conditions for evaluating the vehicle-bridge interactions. The primary suspension system between each wheel-axle

set and the corresponding side frame, having stiffness, k_{yp}, and secondary suspension system between each side frame and the carbody, having stiffness, k_{ys}, were considered as linear springs in series, and were combined to provide an equivalent stiffness, $k_y = 1/(\frac{1}{k_{yp}} + \frac{1}{k_{ys}})$. Various dampings in the suspension systems were also combined in a similar fashion to provide an equivalent damping.

Couplings between the idealized vehicles were assumed to be provided by universal joints. It was further assumed that the wheels (unsprung mass) and rails were always in contact, so that no wheel lifts occurred.

2.3 Equation of Motion for the Bridge

The free vibrational motion of the bridge model, producing deflections due to inertia forces in the lumped masses, is given, using D'Alembert's principle of dynamic equilibrium, as:

$$[M]\ \{\ddot{D}\} + [C]\ \{\dot{D}\} + [K]\ \{D\} = \{0\} \qquad (1)$$

where:

$[M]$ = diagonal mass matrix;

$[C]$ = damping matrix = $a\omega_1\ [M]$

where: a = percentage of critical damping and

ω_1 = fundamental circular frequency;

$[K]$ = stiffness matrix of the bridge structure;

$\{D\}$ = joint displacement vector, representing the displaced shape of the structure

= $[v_1, v_2, ----, v_n]^T$, where v_i is the retained vertical displacement of the ith node or joint;

$\{\dot{D}\},\{\ddot{D}\}$ = first and second derivatives of $\{D\}$, with respect to time, representing the joint velocity vector and joint acceleration vector, respectively;

$\{0\}$ = null vector.

In the case of interactive (forced) vibrations of the bridge structure, the null vector $\{0\}$ is replaced by the resultant interaction vector for the applied nodal loads, including the inertial interaction generated at the various wheel-rail contact points due to the relative accelerations between the sprung mass of each vehicle and the bridge structure.

2.4 Equations of Motion for each Vehicle

Let v_b^i be the displacement, associated with the ith wheel at any time, t. The damped equations of motion for each vehicle, Figures 3 and 4 in Appendix A, are expressed [9] as:

$$M_b\ddot{y}_b + \sum_{i=1}^{n} \{c_y(\dot{y}_b \pm \ell_i\dot{\phi}_b \pm b\dot{\theta}_b - \dot{v}_b^i)+k_y(y_b \pm \ell_i\phi_b \pm b\theta_b - v_b^i)\}=0 \quad (2)$$

$$I_b\ddot{\phi}_b + \sum_{i=1}^{n} \{c_y(\dot{y}_b \pm \ell_i\dot{\phi}_b \pm b\dot{\theta}_b - \dot{v}_b^i)+k_y(y_b \pm \ell_i\phi_b \pm b\theta_b - v_b^i)\} \quad (3)$$
$$(\pm\ell_i) = 0$$

$$J_b\ddot{\theta}_b + \sum_{i=1}^{n} \{c_y(\dot{y}_b \pm \ell_i\dot{\phi}_b \pm b\dot{\theta}_b - \dot{v}_b^i)+k_y(y_b \pm \ell_i\phi_b \pm b\theta_b - v_b^i)\} \quad (4)$$
$$(\pm b) = 0$$

where:

M_b = mass of the carbody and trucks, i.e. the sprung mass;

I_b = pitch moment of inertia of the carbody and trucks;

J_b = roll moment of inertia of the carbody and trucks;

y_b = bounce (vertical displacement) of the vehicle;

ϕ_b = pitch of the vehicle about the transverse axis;

θ_b = roll of the vehicle about the longitudinal axis;

k_y = equivalent vertical suspension stiffness of each wheel;

c_y = equivalent vertical suspension damping of each wheel;

b = one-half of the lateral distance between the wheel set contact points;

ℓ_i = longitudinal distance of the ith wheel from the centroid of the carbody and trucks;

n = total number of wheels in the vehicle;

$(\dot{}), (\ddot{})$ = first and second derivatives with respect to time, respectively.

The sign on ℓ_i and b must be consistent with the pitch and roll movements at each particular instant of time.

2.5 Interactive Forces

The total reaction, F^i, generated at the interface between the rail and the ith wheel, is given [9] by:

$$F^i = M_u(g - \ddot{v}_b^i) + k_y(y_b \pm \ell_i\phi_b \pm b\theta_b - v_b^i) + M_s g \qquad (5)$$

where:

M_u = one-half of the mass of each wheel-axle set (unsprung mass);

$M_s = M_b / n$,

g = acceleration due to gravity.

2.6 Coupled Vehicle/Bridge Equation of Motion

Combining Equations (1) through (5), the following interactive coupled equation of motion for a single vehicle on the bridge structure is obtained.

$$[M]_R \begin{bmatrix} \ddot{D} \\ \{\ddot{y}_b \ddot{\phi}_b \ddot{\theta}_b\}^T \end{bmatrix} + [C]_R \begin{bmatrix} \dot{D} \\ \{\dot{y}_b \dot{\phi}_b \dot{\theta}_b\}^T \end{bmatrix} + [K]_R \begin{bmatrix} D \\ \{y_b \phi_b \theta_b\}^T \end{bmatrix} = \{F\}_R \quad (6)$$

where:

$[M]_R$ = mass matrix of the coupled vehicle/bridge system;

$[C]_R$ = damping matrix of the coupled vehicle/bridge system;

$[K]_R$ = stiffness matrix of the coupled vehicle/bridge system;

$\{F\}_R$ = interacting nodal force vector of the coupled vehicle/bridge system;

$\{D\}$ = joint displacement vector, representing the displaced structure in the vehicle/bridge system;

$\{y_b \phi_b \theta_b\}^T$ = vector of the bounce, pitch and roll movements of the vehicle.

For more than one vehicle on the bridge, the above equation of motion should be modified, by replacing the vector $\{y_b \phi_b \theta_b\}^T$ with the expanded vector $\{y_{b_1}\ \phi_{b_1}\ \theta_{b_1}\ y_{b_2}\ \phi_{b_2}\ \theta_{b_2}\ --\}^T$, where the subscripts refer to the total number of vehicles on the bridge. Similar expressions should also be applied to those vectors with time derivatives.

3.0 ASSUMPTIONS AND METHOD OF SOLUTION

The method of analysis assumed a linear relationship between the applied loads and the resulting displacement of the structure, so that the principle of superposition was valid. Consequently, the material of the structure obeyed Hooke's Law and was not stressed beyond its elastic limit, implying, therefore, that the change in geometry, due to the imposed deformations, was neligible when compared to the original geometry of the model.

Secondary effects, due to rigidity in the truss's structural joints, were neglected. The shear center of each cross-section was also assumed to coincide with the centroid of the cross-section, and the effects of rotatory inertia were neglected.

The model used in the simulation had limitations on both the number of vehicles in the train and the number of tracks on the bridge. The model limited the total number of vehicles to six, and it was assumed that this limit would fairly well represent the actual conditions on the majority of reasonably long spans. The model also limited the number of tracks on the bridge to two and this was thought to be representative of a large number of actual bridges. Only the vehicle in its normal operating condition was considered, and the effects of vehicle truck hunting or braking, resulting in lateral or longitudinal motions of the bridge, were neglected.

The bridge structure was assigned two degrees-of-freedom for each joint: the vertical and longitudinal displacements. Only the vertical motions of the nodes were retained for calculations in the equations of motion. The other degrees-of-freedom; i.e., the longitudinal components of the nodal displacements, were accounted for by employing the dynamic

condensation scheme. This resulted in reduced orders of the mass, stiffness and damping matrices, and was both computationally efficient and economical.

The interaction between the bridge and the vehicle(s) was expressed by the motion of each vehicle's unsprung mass, which was obtained from the adjacent bridge joint displacements. Linear interpolation was used to express the displacement, v_b^i, of the bridge which was associated with the ith wheel of the vehicle at any time, t.

If the ith wheel was assumed to be located on the track segment lying between the kth (or k′th) and (k+1)th (or (k′+1)th) joints, Figures 4 and 5 in Appendix A, then v_b^i was expressed, as follows:

$$v_b^i = \bar{\lambda}(\alpha_i v_{k+1}^i + \beta_i v_k^i) + \lambda(\alpha_i v_{k'+1}^i + \beta_i v_{k'}^i), \text{ and} \qquad (7)$$

$$\ddot{v}_b^i = \bar{\lambda}(\alpha_i \ddot{v}_{k+1}^i + \beta_i \ddot{v}_k^i) + \lambda(\alpha_i \ddot{v}_{k'+1}^i + \beta_i \ddot{v}_{k'}^i) \qquad (8)$$

where:

$\alpha_i = x_i/\ell_p$

$\beta_i = 1-\alpha_i$

$\lambda = d_1/c$

$\bar{\lambda} = 1-\lambda$

x_i = distance of the ith wheel from the kth or k′th joint;

ℓ_p = length of the beam segment, or panel length of the loaded chord;

d_1 = distance of the nearest rail of the closest track to the centerline of the girder or truss;

c = center-to-center distance between girders or trusses;

$v_k, v_{k+1}, v_{k'}, v_{k'+1}$ = bridge joint displacements, associated with the ith wheel.

For the (i+1)th wheel, the value, d_1, was changed to d_1', and λ and $\bar{\lambda}$ were changed to ξ and $\bar{\xi}$, respectively, so that:

$$v_b^{i+1} = \bar{\xi}(\alpha_{i+1} v_{k+1}^{i+1} + \beta_{i+1} v_k^{i+1}) + \xi(\alpha_{i+1} v_{k'+1}^{i+1} + \beta_{i+1} v_{k'}^{i+1}), \quad (9)$$

and

$$\ddot{v}_b^{i+1} = \bar{\xi}(\alpha_{i+1} \ddot{v}_{k+1}^{i+1} + \beta_{i+1} \ddot{v}_k^{i+1}) + \xi(\alpha_{i+1} \ddot{v}_{k'+1}^{i+1} + \beta_{i+1} \ddot{v}_{k'}^{i+1}) \quad (10)$$

where:

$\xi = d_1'/c$;

$\bar{\xi} = 1-\xi$

d_1' = distance of the farthest rail of the closest track to the centerline of the girder or truss;

$\alpha_{i+1} = \alpha_i$

$\beta_{i+1} = \beta_i$

$v_k^{i+1} = v_k^i$;

$v_{k+1}^{i+1} = v_{k+1}^i$

$v_{k'}^{i+1} = v_{k'}^i$

$v_{k'+1}^{i+1} = v_{k'+1}^i$

Similar linear interpolations were used to calculate the interacting forces, generated at the interfaces between the rail and the ith and (i+1)th wheels, at the nodes of the associated track segment. That is:

$$\left.\begin{aligned} F_k^i &= \beta_i \bar{\lambda} F^i \\ F_{k+1}^i &= \alpha_i \bar{\lambda} F^i \\ F_{k'}^i &= \beta_i \lambda F^i \\ F_{k'+1}^i &= \alpha_i \lambda F^i \end{aligned}\right\} \quad \text{, and} \qquad (11)$$

$$\left.\begin{aligned} F_k^{i+1} &= \beta_i \bar{\xi} F^{i+1} \\ F_{k+1}^{i+1} &= \alpha_i \bar{\xi} F^{i+1} \\ F_{k'}^{i+1} &= \beta_i \xi F^{i+1} \\ F_{k'+1}^{i+1} &= \alpha_i \xi F^{i+1} \end{aligned}\right\} \qquad (12)$$

4.0 DESCRIPTION OF FIELD TESTS AND DATA

The only test results used for comparison with the analytical model were obtained from field investigations of truss-bridge spans, conducted by the Association of American Railroad's (AAR) Research Center, in collaboration with the American Railway Engineering Association (AREA) Committee 30, entitled, "Impact and Bridge Stresses" [4,5]. The purpose of these field investigations was to determine the static stresses, maximum stresses, roll effects, total impacts and frequency of maximum stress occurrences in various bridge members.

4.1 Description of Test Bridges and Spans

4.1.1 Priest River Bridge [4]

This bridge, located on the former Great Northern Railway in Idaho, and consisting of a 200 ft. span carrying a single tangent track, was built in 1954. It is a Warren-type, through-truss span with an open deck, composed of eight, 25 ft. panels. The trusses are spaced 19 ft., 4 in. on centers. The open deck is supported on stringers which are 7 ft., 6 in. on centers. The design was based on a Cooper's E65 live load, using as an impact: $I = 300/(300 + L^2/100)$. Basic design stresses of 16,000 psi in tension, and (15,000 - 50 ℓ/r) psi in compression, were used; ℓ/r being the slenderness ratio for the compression member.

4.1.2 Devil's River Bridge [5]

This bridge, located on the Southern Pacific in Texas, and consisting of two, 300 ft. spans and four, 400 ft.

spans to carry a single tangent track, was built in 1963. All spans are curved-chord, Warren-type, through-trusses with ballasted decks. The trusses are spaced 22 ft. on centers. The steel plate ballasted decks are carried on transverse beams, spaced 2 ft., 6 in. on centers, and on longitudinal stringers, spaced 7 ft. center-to-center. The design was based on a Cooper's E72 live load, using an impact based upon the 1958 AREA Specifications. Basic design stresses of 18,000 psi, for the A7 steel in the stringers, floor beams and hangers, and of 24,000 psi, for the A440 steel in the main truss members, were used.

4.2 Test Train and Test Procedures

The Cooper's Equivalent of the test trains, based on the maximum moment in the span, was E37 for the Priest River Bridge, and E59.8 and E61.2 for the 300 ft. and 400 ft. spans, respectively, in the Devil's River Bridge. The test train data for both bridges is shown in Tables 1 and 2 in Appendix B.

The instrumentation included oscillographs to record the strain gage responses, that were used to determine the stresses, and devices, such as spring-type switches or wheel trips, that were used to determine the relative positions of the wheels on the span. The various train speeds were determined by the use of electric timers, activated by switches that were located a known fixed distance apart on the span.

The strain gages on the chords, diagonals and end posts were located in pairs near the mid-length of each member and along the neutral axis, so as to record only the direct

stresses and eliminate all secondary effects. The gages on the hangers were located above the floor beam knee brace, where the combined direct and bending stresses were high. They were also located at mid-span on the tension flanges of the stringers, and at mid-span, on either the tension flanges or the compression flanges, of the floor beams.

During the actual field test procedures, the first phase was conducted to determine the frequencies of occurrence of the maximum stresses from regular service trains. Impact data was then obtained by operating the test trains on the spans over a wide range of speeds during the second phase.

4.3 Test Results

A detailed discussion of the test results is deferred here and only the salient features of these test studies are included in this report. For detailed tables and plots of these test results, the reader is referred to References [4] and [5]. As earlier mentioned in this Section, the purpose of these tests was to evaluate the static stresses, maximum stresses, roll effects, total impacts and the frequency of maximum stress occurrences in the various bridge members.

A comparison of measured and calculated static stresses for the various bridge members revealed that the bottom chord, floor beams and, to a lesser degree, the stringers made up, significantly, an interacting system such that the bottom chord interacted with the floor system, and floor beams and stringers interacted with the ballast floor plate. Measured values for hangers, which included bending, were about 40 to 50% higher than the calculated values.

All of the equivalent roll percentages at the rail center were either within or in the immediate neighborhood of the AREA's design recommendations of 20%. There was a general trend toward a slight increase in roll with an increase in speed at the lower speed ranges. The results were too scattered for generalization, however, it was still concluded that there was an increase

in roll effects with increasing train speed, since higher rolls occurred at higher train speeds.

All of the measured impact values for the various bridge members were well within the limits of the AREA recommendations for rolling loads without hammer blows. Higher impacts at higher speeds were evident, and this trend was particularly so in the case of the stringers, floor beams and hangers.

Measured maximum stresses were well within the calculated values derived from the calculated test train static values plus the AREA impacts. The maximum measured hanger stresses were of the order of 135% of the stresses calculated with the AREA's Impact Formula. This depicted a very strong bending influence which amounted to as much as 81% of the average stress in the 300 ft. span, and 52% in the 400 ft. span, of the Devil's River Bridge. An increase in stress with speed was most apparent in the hangers, floor beams and stringers. For stringers, the measured stresses were higher under the cars than the locomotives.

Test results for frequency of maximum stresses revealed that the stresses under the locomotives and cars were predominantly less than 54% of the maximum occurrences, except in the case of stringers under locomotives on the 300 ft. span, where 75% were in the 4 to 5 ksi range, which was the average of the total effective stress range. The maximum occurrences were either in the low range, or in the average to intermediate range of stress. Only 2% or less occurrences were near the maximum stress range.

5.0 COMPARISON OF TEST AND MODEL RESULTS

The amplification factors, Λd and Λs, for dynamic (Γd) and static (Γs) responses, respectively, are defined as follows:

$$\Lambda d = \Gamma d/\Gamma_{sm} \text{ and}$$

$$\Lambda s = \Gamma s/\Gamma_{sm}$$

where: Γ_{sm} is the maximum static response.

The impact factor, I, is defined as follows:

$$I = \{Max|\Lambda d|-1\}$$

A model analysis was performed on the Priest River and Devil's River Bridges, both of which were described previously in Section 4.0. These bridges were subjected to a train of four-axle vehicles, moving at speeds between 30mph and 70 mph. The model train for the 200 ft. Priest River Bridge span consisted of two locomotives and two cars, and that for the 300ft. Devil's River Bridge span, two locomotives and four cars. The vehicle's suspension stiffness per wheel was 7000 lbs. per in. for locomotives, and 11200 lbs. per in. for cars. Initial bounce and roll conditions were assumed to be 1/2 in. and 0.04 radians, respectively, in order to reflect normal operating conditions. Results were evaluated for no initial conditions, and for the simultaneous applications of both of these conditions on all the vehicles in the train. These conditions were specified at the time of the entry of each vehicle on the span. The present analysis discounted any presence of structural damping in the bridge system.

5.1 Model Results

Plots for stress and deflection impacts, presented in Appendix D, show only the maximum (envelope) values at the various discrete speeds, which are joined by straight lines, only for the sake of simplicity. It should be noted that it is entirely possible that maximum values may have occurred at some particular speed in the interval between any two discrete speed values

used in the analysis. These discrete maximum values were extracted, for similar members, from either of the trusses (near side and far side trusses) for the particular speeds. It should, therefore, be noted that the minimum values noted in these plots might not be the absolute minimum values at that speed, as given by this model for that particular member or node. One should refer to the Tables in Appendix C for the absolute minimum values. Also the symmetry of the bridge geometry was recognized, in the sense that the impact extremums were picked up, for a particular node, from all of the nodal impact results at the nodes, which were symmetrically located with respect to the center line of the bridge geometry.

5.1.1 Impact in Terms of Member Stresses

A. Priest River Bridge

The model results are given in Tables 3 and 4 in Appendix C, and illustrated, together with test envelope-curves and AREA-specified limits, in Figures 6 through 10 in Appendix D. Analytical curves are plotted using the maxima of the impact values for a certain speed from either of the trusses, i.e., the near-side truss or the far-side truss, to correctly depict the maximum variations in the impact values.

The impact factor becomes negative when the dynamic stress is less than the static stress for a certain bridge member. Neglecting such values, the variations of impact factors, based only on axial stresses, are as follows:

A1. Without Initial Conditions

i) Bottom Chord

Minimum impact of 0.78% at 30 mph to maximum impact of 2.23% at 50 mph, with a median (average) value of 1.24%.

ii) Top Chord

Minimum impact of 1.26% at 30 mph to maximum impact of 3.29% at 50 mph, with a median value of 2.31%.

iii) **Hangers**

Minimum impact of 5.77% at 30 mph to maximum impact of 12.02% at 60 mph, with a median value of 8.92%.

iv) Diagonals

Minimum impact of 2.26% at 60 mph to maximum impact of 8.25% at 40 mph, with a median value of 5.13%.

v) End Posts

Minimum impact of 3.07% at 30 mph to maximum impact of 5.11% at 50 mph, with a median value of 3.84%.

A2. With Initial Conditions

i) Bottom Chord

Minimum impact of 3.53% at 70 mph to maximum impact of 12.14% at 30 mph, with a median value of 6.56%.

ii) Top Chord

Minimum impact of 3.80% at 60 mph to maximum impact of 9.47% at 30 mph, with a median value of 7.25%.

iii) Hangers

Minimum impact of 4.76% at 50 mph to maximum impact of 24.59% at 40 mph, with a median value of 11.99%. It should be mentioned here that at 70 mph, for this particular bridge, the dynamic force became less than the static value. The average value of 11.99% was, therefore, calculated excluding the 70 mph speed.

iv) Diagonals

Minimum impact of 2.34% at 60 mph to maximum impact of 20.25% at 30 mph, with a median value of 10.25%.

v) End Posts

Minimum impact of 1.81% at 70 mph to maximum impact of 12.0% at 40 mph, with a median value of 6.54%.

B. Devil's River Bridge

The model results are given in Tables 5 and 6 in Appendix C, and illustrated, together with test envelope-curves and AREA-specified limits, in Figures 11 through 15 in Appendix D. As mentioned in Section 5.1.1, only the maximum values from either of the trusses is depicted. The variations of impact factors are as follows:

B1. Without Initial Conditions

i) Bottom Chord

Minimum impact of 0.87% at 40 mph to maximum impact of 2.6% at 70 mph, with a median value of 1.61%.

ii) Top Chord

Minimum impact of 1.61% at 40 mph to maximum impact of 5.3% at 60 mph, with a median value of 3.1%

iii) Hangers

Minimum impact of 7.63% at 30 mph to maximum impact of 19.16% at 60 mph, with a median value of 13.2%.

iv) Diagonals

Minimum impact of 2.95% at 60 mph to maximum impact of 7.25% at 50 mph, with a median value of 4.18%.

v) End Posts

Minimum impact of 1.61% at 40 mph to maximum impact of 5.3% at 60 mph, with a median value of 3.1%.

B2. With Initial Conditions

i) Bottom Chord

Minimum impact of 4.87% at 30 mph to maximum impact of 18.35% at 50 mph, with a median value of 11.4%.

ii) Top Chord

Minimum impact of 3.62% at 30 mph to maximum impact of 16.9% at 70 mph, with a median value of 11.7%. It should also be noted that an impact of 16.3% occurred at 40 mph.

iii) Hangers

Minimum impact of 0.85% at 70 mph to maximum impact of 29.87% at 40 mph, with a median value of 19.1%. Also note that the impact values were 26.36% and 27.89% at 50 mph and 60 mph, respectively.

iv) Diagonals

Minimum impact of 0.17% at 60 mph to maximum impact of 18.55% at 70 mph, with a median value of 11%.

v) End Posts

Minimum impact of 4.9% at 30 mph to maximum impact of 17.67% at 60 mph, with a median value of 11%. Also note that the impact at 40 mph was 17.43%.

5.1.2 Impacts in Terms of Nodal Delfections

The analytical results are given in Tables 3 through 6 in Appendix C, and are plotted in Figures 16 and 17 in Appendix D.

Impacts, in terms of deflections, were presumed to be the aggregate (average) responses at the node locations. A comparison with stress-impacts showed that deflection-impacts were comparatively smaller at all speed values and for either of the prescribed initial condition cases. It was further to be noted that the variation of these impacts across the speed range was much smoother compared to the stress-impacts. The two extremums and the average value for various nodes are as follows:

A. Priest River Bridge

A1. Node No. 2

i) Without Initial Conditions.

Minimum impact of 1.12% at 30 mph to maximum impact of 3.9% at 70 mph, with a median value of 2.48%.

ii) With Initial Conditions

Minimum impact of 4.3% at 60 mph to maximum impact of 12.01% at 70 mph, with a median value of 8.0%.

A2. Node No. 4

i) Without Initial Conditions

Minimum impact of 1.21% at 30 mph to maximum impact of 3.13% at 50 mph, with a median value of 1.92%.

ii) With Initial Conditions

Minimum impact of 4% at 60 mph to maximum impact of 10.13% at 30 mph, with a median value of 6.82%.

B. Devil's River Bridge.

B1. Node No. 2

i) Without Initial Conditions

Minimum impact of 0.25% at 70 mph to maximum impact of 3.67% at 70 mph, with a median value of 1.42%.

ii) With Initial Conditions

Minimum impact of 2.98% at 30 mph to maximum impact of 17.32% at 70 mph, with a median value of 10.74%.

B2. Node No. 3

i) Without Initial Conditions

Minimum impact of 0.68% at 40 mph to maximum impact of 3.48% at 60 mph, with a median value of 1.78%.

ii) With Initial Conditions

Minimum impact of 3.1% at 30 mph to maximum impact of 17.56% at 50 mph, with a median value of 10.5%.

B3) Node No. 5

i) Without Initial Conditions

Minimum impact of 0.93% at 30 and 40 mph to maximum impact of 2.42% at 70 mph, with a median value of 1.52%.

ii) **With Initial Conditions**

Minimum impact of 4.5% at 30 mph to maximum impact of 18.53% at 50 mph, with a median value of 10.9%.

5.2 Comparison with Test Data and AREA Limits

During the tests, it was assumed that the total measured impacts included effects from the roll, speed and track geometry, as these conditions actually existed at the bridge sites. The model results were, on the other hand, evaluated using prescribed initial displacement conditions on the vehicles. These model results, therefore, deal with only a very limitied portion of the actual test environment. However, the inclusion of roll effects and their magnitudes in the total measured impact values from the tests is doubtful, since the specific roll conditions for all of the vehicles in each train consist during the testing activities were not known. Moreover, out-of-phase roll conditions in contiguous vehicles in the train consist might have cancelled the prominence of this effect. It is further emphasized that the Devil's River Bridge had a ballasted deck, so that AREA impact values should be reduced to 90%, due to the damping nature of this deck. However, since structural damping was neglected in the analysis, in the model results reported here this bridge was treated as a deck bridge, although the additional mass of the ballast floor was accounted for by lumping the masses at the nodes. For a comparison with the AREA limits for this bridge, the AREA values would, therefore, not be reduced to 90%, as required by code, and the full 100% values should be used instead.

The comparison was based, therefore, on the qualification of the above premise, such that it was not on a point-by-point basis, but only to cover a range. This is discussed below.

5.2.1 Priest River Bridge

The AREA-specified limits and the maximum test values, together with the

maximum analytical values are given in Table 7 in Appendix C.

A comparison showed that the model values were only 68% (or lower) of the specified AREA limits for this bridge. However, a comparison with test values showed that, except in the case of a bottom chord, all other test values were lower than the model results. In the case of the bottom chord this test value was 114% of the model result. It should further be noted that except for diagonals, where the difference was 171%, other test results compared favorably with the model results, such that these differences were 75%, 65% and 4% for the top chord, hangers and end posts, respectively.

5.2.2 Devil's River Bridge

The AREA-specified limits and the maximum test values, together with the maximum analytical values, are given in Table 7 in Appendix C.

A comparison showed that the model values were only 81% (or lower) of the specified AREA limits for this bridge. However, a comparison with test values showed that, except in the case of a hanger, all other test values were lower than the model results. In the case of the hanger this test value was 111% of the model result. The overall test results compared favorably with the model values, except in the case of diagonals where the difference was 108%.

6.0 CONCLUSIONS

A method was developed to analyze the dynamic response of coupled vehicle(s)/girder or vehicle(s)/truss bridge systems. The bridge was considered as a lumped-mass system of two planar structures, interconnected by a rigid and simply supported floor system. Each vehicle was idealized as a four or six axle, sprung rigid-body, with three degrees-of-freedom: bounce, pitch and roll. The suspension system was reduced to a vertical spring between the vehicle body and each wheel. The variations in displacement, velocity, acceleration and interactive force between any two consecutive nodes were assumed to be linear. The resulting coupled equations of motion were solved, using the Central Difference numerical method, for the two truss bridges used in the analysis.

The limitations of the present analysis were discussed in detail in Section 2.0 and 3.0. Within these limitations, the results for the designated truss elements and truss nodes have been presented and compared with the test results in Section 5.0. It is further emphasized that this model analysis represents only a very limited portion of the actual field environment, such that only two specific truss bridges have been used for comparison with the analytical results. Also, only a very limited number of parameters, out of a much larger number of actual parameters, were included in this analysis.

In light of all of the assumptions used in these general discussions, the various conclusions are as follows:

1) Impact did not necessarily increase with the increase in train speed. Maximum impact seemed to occur at certain speeds, depending on the particular characteristics of the bridge component and the nature of the bridge under consideration, as follows:

i) Without Initial Conditions

A. Priest River Bridge: The maximum impact value for the bottom chord, top chord and end posts occurred at 50 mph. For hangers and diagonals this value occurred at 60 mph and 40 mph, respectively.

B. Devil's River Bridge: Impact seemed to gradually increase to a maximum value at 70 mph, for both the bottom chord and top chord. For hangers, the maximum value occurred at 60 mph; however at 50 mph the value of impact was quite comparable with the maximum value. For diagonals and end posts, maximum values occurred at 50 mph and 60 mph, respectively.

ii) With Initial Conditions

A. Priest River Bridge: Maximum impact values occurred at 30 mph (gradually decreasing with an increase in speed) for the bottom chord, at 30 and 70 mph for the top chord, at 40 mph for the hangers, at 30 mph (with comparable value at 70 mph) for the diagonals and at 40 mph (gradually decreasing with increase in speed) for the end posts.

B. Devil's River Bridge: Maximum impact values occurred at 50 mph for the bottom chord, at 40 mph (with comparable value at 50 mph) for the top chord, at 40 mph for the hangers, at 40 mph (impact value at 70 mph being greater) for the diagonals and at 40 and 60 mph (with comparable value at 50 mph) for the end posts.

2) The inclusion of "initial conditions," such as bounce and roll motions of the vehicle at the time of entry onto the bridge, generally magnified appreciably the resulting impact effects.

3) The model analysis may not correctly depict actual hanger behavior, since only direct stresses were used in the analysis, whereas an actual hanger having offset end connections is always subjected to the duality of both direct and bending stresses. However, a comparison of the test results with the corresponding "no initial condition" analytical results would require the

inclusion of compatible initial conditions in the analysis, in order to explain the generation of higher hanger impacts at the higher test speeds. It was apparent that, in general, the maximum test values were intermediate between the model's without-initial-conditions and with-initial-conditions maximum values, except in the cases of the bottom chord of the Priest River Bridge and the hangers of the Devil's River Bridge, where the test values exceeded the model values. Also, due to comparable panel lengths on these bridges, the scatter of impact values with respect to speeds for both these bridges was quite similar. It should also be pointed out that, at speeds beyond the maximum-value-speeds, the hanger impacts, for the particular truss bridges used in the analysis, have a tendency to sharply decrease.

4) The maximum analytical values were well within the AREA's specified limits. However, it should be mentioned that there exists other dynamic magnifiers, e.g., battered rail joints, irregular track geometry, etc., the inclusion of which may cause higher impact values than those calculated. It is felt that the limits set by AREA are quite reasonable for the present time.

5) The present model has been, by the use of realistic simplifying assumptions, reduced to a simple one for the preliminary demonstrative purpose. A comparison with actual tests showed that the dispersion of results was not wide. The merit of this model lies in its being simple, without undue compromise on the range of the expected impact values. However, it is felt that to account for variations in the types of bridge construction and geometry; in track structural geometry and track maintenance-related parameters, and in the vehicle dynamics and associated maintenance parameters, a more sophisticated analytical model would be required to suitably conduct parametric studies and obtain more comprehensive results regarding the phenomenon of impact in bridges.

7.0 REFERENCES

1. Dhar, C.L., "A Method of Computing Bridge Impact," Thesis Submitted in Partial Fulfillment of the Requirements for a Doctor of Philosophy Degree at the Illinois Institute of Technology, Chicago, Illinois, May, 1978.

2. Dhar, C.L., Chu, K.H., and Garg, V.K., "Dynamic Response of a Single Track Truss Bridge," Paper Presented at the National Bridge Engineering Conference, Sponsored by the Transportation Research Board at St. Louis, MO., September 25-27, 1978.

3. American Railway Engineering Association, Manual for Railway Engineering, Chicago, Illinois, 1973, Chapter 15. "Steel Structures."

4. Association of American Railroads, "Field Investigation of a Truss Span on the Great Northern Railway," Report No. ER-81, Chicago, Illinois, May, 1968.

5. Association of American Railroads, "Field Investigation of Two Truss Spans on the Southern Pacific Company," Report No. ER-82, Chicago, Illinois, May, 1968.

6. Willis, R., "Appendix of the Report of Commissioners Appointed to Inquire into the Application of Iron to Railway Structures," His Majesty's Stationary Office, London, 1849.

7. Timoshenko, S., "Vibration of Bridges," ASME (American Society of Mechanical Engineers) Transactions, V.53, 1928. See also Vibration Problems in Engineering, D. Van Nostrand Company, Princeton, N.J.,1955.

8. Inglis, C.E., "Mathematical Treatise on Vibration of Railway Bridges," Cambridge University Press, London, 1932.

9. Biggs, J.M., Introduction to Structural Dynamics, McGraw-Hill Book Company, New York, New York, 1964.

8.0 APPENDICES

8.1 Appendix A

Bridge and Vehicle Models

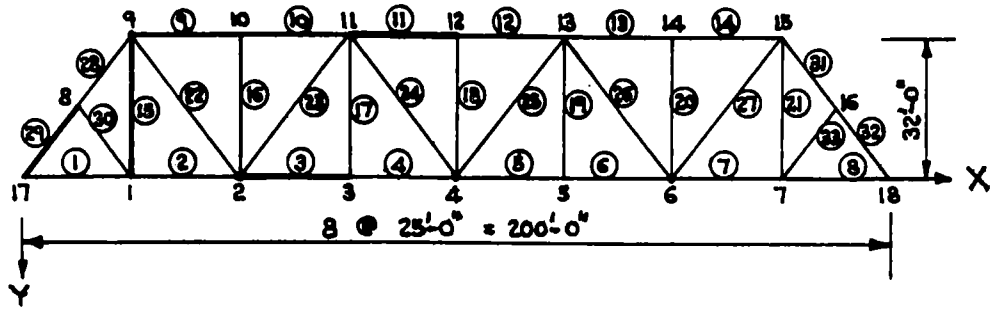

LEGEND: Members and nodes in bold graphics represent those locations for impact evaluation in the analysis.

NOTE: This Figure shows the near-side truss. The far-side truss joint and member numbers follow a similar numbering scheme, starting from the last number of the corresponding component in the near-side truss.

Figure 1. Great Northern Bridge (Bridge #3 in the Analysis) Joint and Member Numbers and Coordinates.

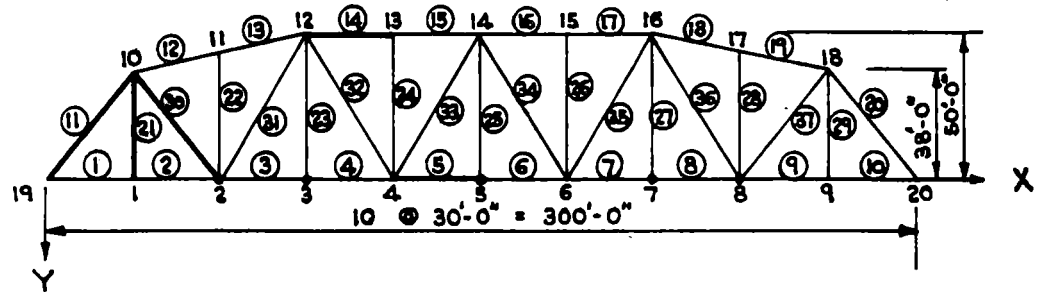

LEGEND: Members and nodes in bold graphics represent those locations for impact evaluation in the analysis.

NOTE: This Figure shows the near-side truss. The far-side truss joint and member numbers follow a similar numbering scheme, starting from the last number of the corresponding component in the near-side truss.

Figure 2. Southern Pacific Bridge (Bridge #4 in the Analysis) Joint and Member Numbers and Coordinates.

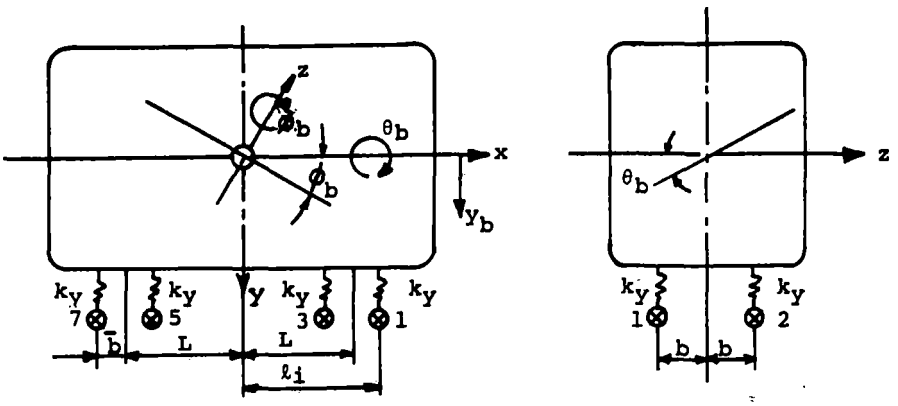

Figure 3. Idealized Vehicle Model.

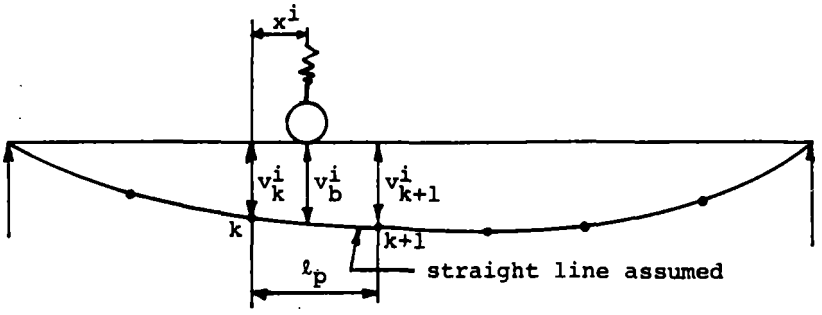

Figure 4. Side View Showing the Relationship of the Deflection Under a Wheel to the Deflections at Neighboring Nodes.

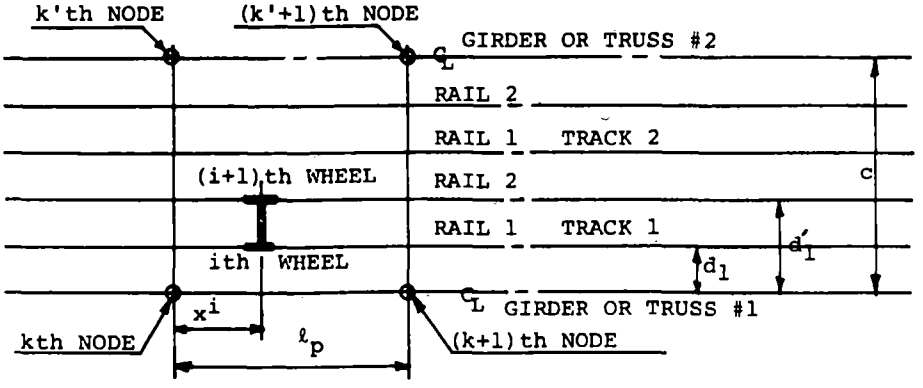

Figure 5. Plan View of the Position of a Wheel Load in a Typical Bridge Panel.

8.2 Appendix B

Test Train Data for the Great Northern

and Southern Pacific Bridge Tests

Table 1. Test Train Data for Great Northern Railway Bridge No. 244

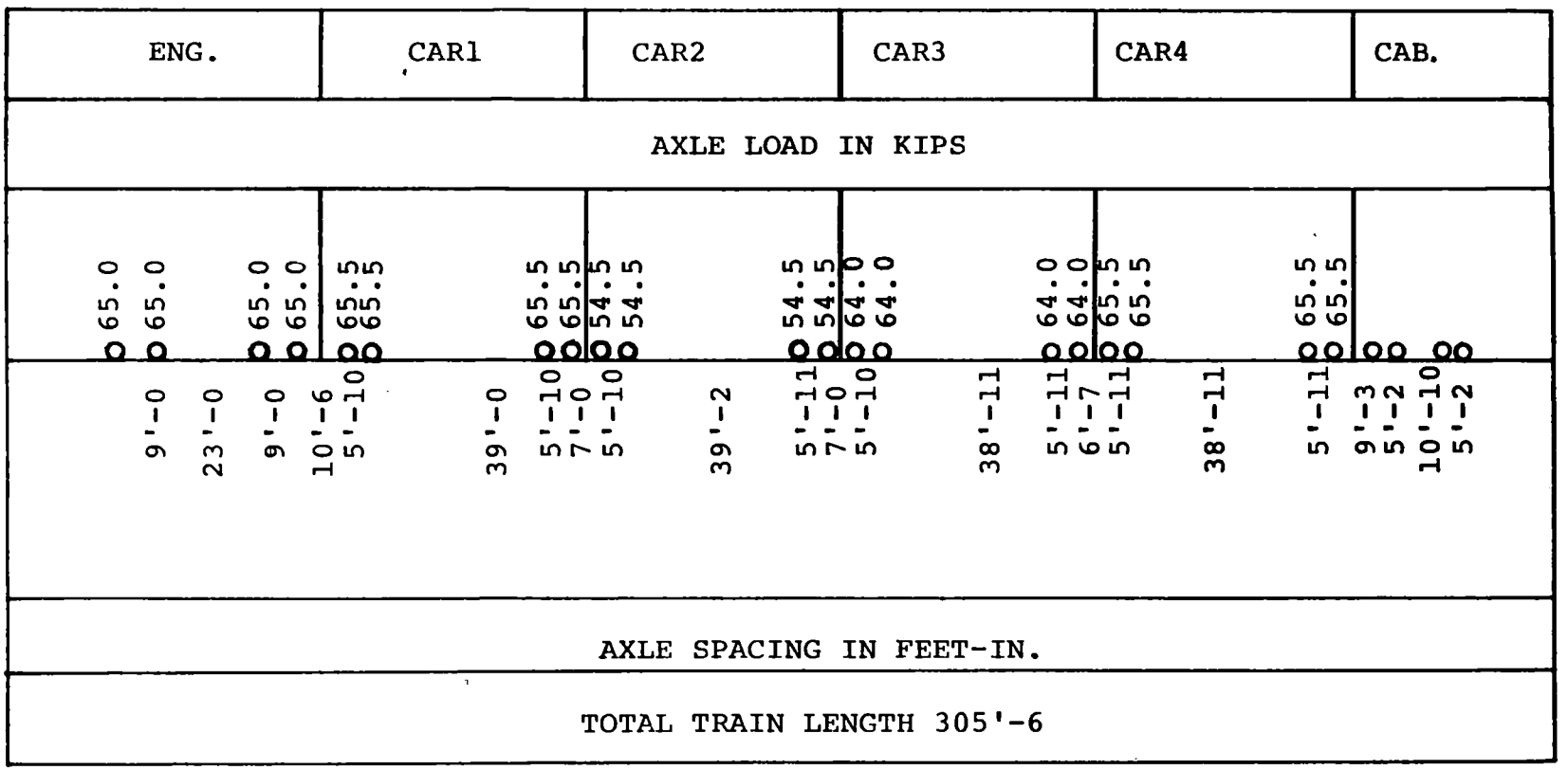

Table 2. Test Train Data for Southern Pacific Bridge No. 393.14

300' SPAN-RUNS 53 TO 86 INCLUSIVE

	Eng. 7415	Eng. 7737	Car 1	Car 2	Car 3	Car 4	Car 5	Car 6	Car 7	Car 8	Car 9	Car 10	Cab.
Axle loads	66.0 66.0 66.0 66.0	65.8 65.8 65.8 65.8	56.6 56.6 56.6 56.6	55.2 55.2 55.2 55.2	55.8 55.8 55.8 55.8	55.1 55.1 55.1 55.1	59.6 59.6 59.6 59.6	57.5 57.5 57.5 57.5	53.8 53.8 53.8 53.8	56.8 56.8 56.8 56.8	55.5 55.5 55.5 55.5	53.5 53.5 53.5 53.5	

Spacings: 9'-0, 23'-0, 9'-0, 14'-3, 9'-0, 23'-0, 9'-0, 11'-7, 5'-9, 16'-6, 5'-9, 6'-11, 5'-8, 16'-10, 5'-8, 6'-9, 5'-9, 16'-11, 5'-9, 6'-9, 5'-8, 16'-11, 5'-8, 6'-8, 5'-8, 16'-7, 5'-8, 6'-9, 5'-8, 16'-11, 5'-8, 7'-0, 5'-6, 16'-4, 5'-6, 7'-0, 5'-8, 16'-8, 5'-8, 6'-10, 5'-8, 16'-11, 5'-8, 6'-11, 5'-8, 16'-7, 5'-8

300' SPAN-RUNS 88 TO 97 INCLUSIVE

	Cab	Car 1	Car 2	Car 3	Car 4	Car 5	Car 6	Car 7	Car 8	Car 9	Car 10	Eng. 7415	Eng. 7737
Axle loads		56.6 56.6 56.6 56.6	55.2 55.2 55.2 55.2	55.8 55.8 55.8 55.8	55.1 55.1 55.1 55.1	59.6 59.6 59.6 59.6	57.5 57.5 57.5 57.5	53.8 53.8 53.8 53.8	56.8 56.8 56.8 56.8	55.5 55.5 55.5 55.5	53.5 53.5 53.5 53.5	66.0 66.0 66.0 66.0	65.8 65.8 65.8 65.8

Spacings: 5'-9, 16'-6, 5'-9, 6'-11, 5'-8, 16'-10, 5'-8, 6'-9, 5'-9, 16'-11, 5'-9, 6'-9, 5'-8, 16'-11, 5'-8, 6'-8, 5'-8, 16'-7, 5'-8, 6'-9, 5'-8, 16'-11, 5'-8, 7'-0, 5'-6, 16'-4, 5'-6, 7'-0, 5'-8, 16'-8, 5'-8, 6'-10, 5'-8, 16'-11, 5'-8, 6'-11, 5'-8, 16'-7, 5'-8, 11'-7, 9'-0, 23'-0, 9'-0, 14'-3, 9'-0, 23'-0, 9'-0

400' SPAN-ALL RUNS

	Cab	Car 1	Car 2	Car 3	Car 4	Car 5	Car 6	Car 7	Car 8	Car 9	Car 10	Eng. 7706	Eng. 771
Axle loads		56.6 56.6 56.6 56.6	55.2 55.2 55.2 55.2	55.8 55.8 55.8 55.8	55.1 55.1 55.1 55.1	59.6 59.6 59.6 59.6	57.5 57.5 57.5 57.5	53.8 58.8 53.8 53.8	56.8 56.8 56.8 56.8	55.5 55.5 55.5 55.5	53.5 53.5 53.5 53.5	65.9 65.9 65.9 65.9	65.5 65.5 65.5 65.5

Spacings: 5'-9, 16'-6, 5'-9, 6'-11, 5'-8, 16'-10, 5'-8, 6'-9, 5'-9, 16'-11, 5'-9, 6'-9, 5'-8, 16'-11, 5'-8, 6'-8, 5'-8, 16'-7, 5'-8, 6'-9, 5'-8, 16'-11, 5'-8, 7'-0, 5'-6, 16'-4, 5'-6, 7'-0, 5'-8, 16'-8, 5'-8, 6'-11, 5'-8, 16'-11, 5'-8, 6'-11, 5'-8, 16'-7, 5'-8, 11'-7, 9'-0, 23'-0, 9'-0, 14'-3, 9'-0, 23'-0, 9'-0

NOTE: Axle Loads in Kips, Spacing in Feet.
Total Train Weight: 2764.8 Kips
Total Train Length: 449 Feet, 11 Inches.

8.3 Appendix C

Analytical Impact Percentages for Bridge Member Stresses and Nodal Deflections in the Great Northern and Southern Pacific Bridges

Table 3. Analytical Impact Percentages for Member Stresses and Nodal Deflections in the Great Northern Bridge, for a Train of Four-Axle Vehicles (Two Locomotives and Two Cars) With a Wheel Suspension Stiffness of 7,000 Lb./In. for the Locomotives and 11,200 Lb./In. for the Cars. No Initial Vehicle Bounce and Roll Conditions.

NO INITIAL CONDITIONS											
MEMBER[a]	MAX. STATIC STRESS	SPEED = 30 mph		SPEED = 40 mph		SPEED = 50 mph		SPEED = 60 mph		SPEED = 70 mph	
		DYNAMIC STRESS	% IMPACT	DYNAMIC STRESS	% IMPACT	DYNAMIC STRESS	% IMPACT	DYNAMIC STRESS	% IMPACT	DYNAMIC STRESS	% IMPACT
3	3711	3740	0.7768	3772	1.650	3794	2.233	3730	0.5214	3749	1.027
11	-3884	-3932	1.255	-3971	2.241	-4011	3.292	-3978	2.428	-3974	2.334
15	4196	4438	5.772	4613	9.934	4484	6.859	4700	12.02	4616	10.01
22	3970(-166)	-178	7.269	-180	8.248	-172	3.804	4059	2.260	4131	4.051
29	-3687	-3801	3.067	-3828	3.822	-3876	5.113	-3836	4.023	-3804	3.155
36	3711	3740	0.7768	3772	1.650	3794	2.233	3730	0.5214	3749	1.027
44	-3884	-3932	1.255	-3971	2.241	-4011	3.292	-3978	2.428	-3974	2.334
48	4196	4438	5.772	4613	9.934	4484	6.859	4700	12.02	4616	10.01
55	3970(-166)	-178	7.269	-180	8.248	-172	3.804	4059	2.260	4131	4.051
62	-3687	-3801	3.067	-3828	3.822	-3876	5.113	-3836	4.023	-3804	3.155
NODE[a]	MAX. STATIC DISPL.	SPEED = 30 mph		SPEED = 40 mph		SPEED = 50 mph		SPEED = 60 mph		SPEED = 70 mph	
		DYNAMIC DISPL.	% IMPACT	DYNAMIC DISPL.	% IMPACT	DYNAMIC DISPL.	% IMPACT	DYNAMIC DISPL.	% IMPACT	DYNAMIC DISPL.	% IMPACT
2	0.4447	0.4521	1.652	0.4541	2.107	0.4600	3.433	0.4574	2.852	0.4621	3.899
4	0.6443	0.6521	1.209	0.6558	1.775	0.6645	3.126	0.6570	1.973	0.6540	1.497
6	0.4638	0.4690	1.124	0.4734	2.069	0.4799	3.469	0.4748	2.373	0.4725	1.860
20	0.4447	0.4521	1.652	0.4541	2.107	0.4600	3.433	0.4574	2.852	0.4621	3.899
22	0.6443	0.6521	1.209	0.6558	1.775	0.6645	3.126	0.6570	1.973	0.6540	1.497
24	0.4638	0.4690	1.124	0.4734	2.069	0.4799	3.469	0.4748	2.373	0.4725	1.860

NOTE (a): For Identification of the Designated Members and Nodes, See the Bridge Model Shown in Figure 1 of Appendix A.

Table 4. Analytical Impact Percentages for Member Stresses and Nodal Deflections in the Great Northern Bridge, for a Train of Four Axle Vehicles (Two Locomotives and Two Cars) With a Wheel Suspension Stiffness of 7,000 Lb./In. for the Locomotives and 11,200 Lb./In. for the Cars. With Initial Vehicle Bounce and Roll Conditions.

INITIAL CONDITIONS: BOUNCE (EACH VEHICLE) = 0.5 IN., ROLL (EACH VEHICLE) = 0.04 RAD.

MEMBER[a]	MAX STATIC STRESS	SPEED = 30 mph		SPEED = 40 mph		SPEED = 50 mph		SPEED = 60 mph		SPEED = 70 mph	
		DYNAMIC STRESS	% IMPACT	DYNAMIC STRESS	% IMPACT	DYNAMIC STRESS	% IMPACT	DYNAMIC STRESS	% IMPACT	DYNAMIC STRESS	% IMPACT
3	3711	4162	12.14	4063	9.488	3956	6.604	3930	5.913	3842	3.524
11	-3884	-4251	9.468	-4172	7.425	-4121	6.121	-4031	3.802	-4182	7.693
15	4196	4554	8.531	4699	11.99	4450	6.068	4640	10.58	4048	---
22	3970(-166)	-184	10.84	4371	10.11	4376	10.25	4140	4.30	4403	10.91
29	-3687	-3891	5.511	-4117	11.65	-3770	2.231	-3875	5.081	-3754	1.811
36	3711	4009	8.025	3903	5.176	3928	5.856	3877	4.472	3875	4.433
44	-3884	-4235	9.052	-4171	7.387	-4149	6.837	-4118	6.038	-4222	8.717
48	4196	4904	16.89	5228	24.59	4721	12.51	4395	4.756	4094	---
55	3970(-166)	-200	20.25	-179	8.026	4316	8.735	4063	2.34	4636	16.80
62	-3687	-3898	5.705	-4130	12.00	-4040	9.561	-3985	8.074	-3827	3.783

NODE[a]	MAX. STATIC DISPL.	SPEED = 30 mph		SPEED = 40 mph		SPEED - 50 mph		SPEED = 60 mph		SPEED = 70 mph	
		DYNAMIC DISPL.	% IMPACT	DYNAMIC DISPL.	% IMPACT	DYNAMIC DISPL.	% IMPACT	DYNAMIC DISPL.	% IMPACT	DYNAMIC DISPL.	% IMPACT
2	0.4447	0.4967	11.70	0.4895	10.08	0.4874	9.594	0.4654	4.654	0.4888	9.919
4	0.6443	0.7096	10.13	0.6887	6.879	0.6737	4.555	0.6702	4.010	0.6884	6.835
6	0.4638	0.5046	8.782	0.4846	4.481	0.4840	4.355	0.4892	5.462	0.5003	7.857
20	0.4447	0.4874	9.606	0.4869	9.476	0.4778	7.438	0.4821	8.399	0.4981	12.01
22	0.6443	0.6985	8.410	0.6896	7.023	0.6876	6.713	0.6795	5.465	0.6970	8.174
24	0.4638	0.5025	8.332	0.4962	6.973	0.5013	8.081	0.4838	4.307	0.5045	8.775

NOTE (a): For Identification of the Designated Members and Nodes, See the Bridge Model Shown in Figure 1 of Appendix A.

Table 5. Analytical Impact Percentages for Member Stresses and Nodal Deflections in the Southern Pacific Bridge, for a Train of Four-Axle Vehicles (Two Locomotives and Four Cars) With a Wheel Suspension Stiffness of 7,000 Lb./In. for the Locomotives and 11,200 Lb./In. for the Cars. No Initial Vehicle Bounce and Roll Conditions.

NO INITIAL CONDITIONS

MEMBER (a)	MAX. STATIC STRESS	SPEED = 30 mph		SPEED = 40 mph		SPEED = 50 mph		SPEED = 60 mph		SPEED = 70 mph	
		DYNAMIC STRESS	% IMPACT	DYNAMIC STRESS	% IMPACT	DYNAMIC STRESS	% IMPACT	DYNAMIC STRESS	% IMPACT	DYNAMIC STRESS	% IMPACT
5	5470	5527	1.050	5517	0.8708	5564	1.718	5568	1.801	5612	2.599
11	-4070	-4157	2.119	-4136	1.610	-4200	3.196	-4286	5.303	-4199	3.157
14	-4853	-4893	0.8143	-4908	1.129	-4898	0.9245	-4939	1.770	-4948	1.953
21	2613	2812	7.629	2892	10.660	3087	18.120	3114	19.160	2886	10.450
30	4811(-323)	-333	3.067	-334	3.439	4998	3.893	4952	2.947	5014	4.216
42	5470	5527	1.050	5517	0.8708	5564	1.718	5568	1.801	5612	2.599
48	-4070	-4151	2.119	-4136	1.610	-4200	3.196	-4286	5.303	-4199	3.157
51	-4853	-4893	0.8143	-4908	1.129	-4898	0.9245	-4939	1.770	-4948	1.953
58	2613	2812	7.629	2892	10.660	3087	18.120	3114	19.160	2886	10.450
67	4811(-323)	-333	3.067	-334	3.439	4998	3.893	4952	2.947	5014	4.216
NODE (a)	MAX. STATIC DISPL.	SPEED = 30 mph		SPEED = 40 mph		SPEED = 50 mph		SPEED = 60 mph		SPEED = 70 mph	
		DYNAMIC STRESS	% IMPACT	DYNAMIC STRESS	% IMPACT	DYNAMIC STRESS	% IMPACT	DYNAMIC STRESS	% IMPACT	DYNAMIC STRESS	% IMPACT
2	0.7085	0.7144	0.8243	0.7172	1.223	0.7212	1.785	0.7195	1.557	0.7346	3.674
3	1.009	1.022	1.229	1.016	0.6844	1.032	2.272	1.022	1.291	1.036	2.599
5	1.257	1.269	0.9327	1.269	0.9257	1.285	2.172	1.272	1.149	1.288	2.416
7	1.023	1.030	0.7224	1.032	0.9183	1.048	2.487	1.058	3.481	1.044	2.080
8	0.7367	0.7426	0.8047	0.7456	1.209	0.7463	1.303	0.7482	1.556	0.7386	2.487
22	0.7085	0.7144	0.8243	0.7172	1.223	0.7212	1.785	0.7195	1.557	0.7346	3.674
23	1.009	1.022	1.229	1.016	0.6844	1.032	2.272	1.022	1.291	1.036	2.599
25	1.257	1.269	0.9327	1.269	0.9257	1.285	2.172	1.272	1.149	1.288	2.416
27	1.023	1.030	0.7224	1.032	0.9183	1.048	2.487	1.058	3.481	1.044	2.080
28	0.7367	0.7426	0.8047	0.7456	1.209	0.7463	1.303	0.7482	1.556	0.7386	2.487

NOTE (a): For Identification of the Designated Members and Nodes, See the Bridge Model Shown in Figure 2 of Appendix A.

Table 6. Analytical Impact Percentages for Member Stresses and Nodal Deflections in the Southern Pacific Bridge, for a Train of Four-Axle Vehicles (Two Locomotives and Four Cars) With a Wheel Suspension Stiffness of 7,000 Lb./In. for the Locomotives and 11,200 Lb./In. for the Cars. With Initial Vehicle Bounce and Roll Conditions.

INITIAL CONDITIONS: BOUNCE (EACH VEHICLE) = 0.5 IN., ROLL (EACH VEHICLE) = 0.04 RAD.											
MEMBER[a]	MAX. STATIC STRESS	SPEED = 30 mph DYNAMIC STRESS	% IMPACT	SPEED = 40 mph DYNAMIC STRESS	% IMPACT	SPEED = 50 mph DYNAMIC STRESS	% IMPACT	SPEED = 60 mph DYNAMIC STRESS	% IMPACT	SPEED = 70 mph DYNAMIC STRESS	% IMPACT
5	5470	5757	5.249	6325	15.63	5974	9.223	6167	12.75	6333	15.78
11	-4070	-4272	4.945	-4780	17.43	-4363	7.196	-4790	17.67	-4552	11.82
14	-4853	-5029	3.624	-5636	16.12	-5395	11.17	-5461	12.53	-5673	16.89
21	2613	2866	9.694	3321	27.09	2883	10.35	3201	22.49	2560	--
30	4811(-323)	-351	8.529	5382	11.87	5417	12.61	4819	0.170	5703	18.55
42	5470	5736	4.876	6217	13.67	6474	18.35	5847	6.908	6103	11.58
48	-4070	-4276	5.042	-4602	13.06	-4718	15.92	-4386	7.759	-4443	9.142
51	-4853	-5038	3.812	-5642	16.26	-5622	15.85	-5184	6.816	-5532	13.99
58	2613	3076	17.73	3394	29.87	3302	26.36	3342	27.89	2635	0.8523
67	4811(-323)	-361	11.56	5523	14.80	-356	10.03	5027	4.508	5662	17.69
NODE[a]	MAX. STATIC DISPL.	SPEED = 30 mph DYNAMIC DISPL.	% IMPACT	SPEED = 40 mph DYNAMIC DISPL.	% IMPACT	SPEED = 50 mph DYNAMIC DISPL.	% IMPACT	SPEED = 60 mph DYNAMIC DISPL.	% IMPACT	SPEED = 70 mph DYNAMIC DISPL.	% IMPACT
2	0.7085	0.7499	5.839	0.8102	14.36	0.7850	10.79	0.8033	13.38	0.8312	17.32
3	1.009	1.069	5.882	1.166	15.53	1.072	6.23	1.163	15.18	1.159	14.81
5	1.257	1.330	5.787	1.436	14.17	1.357	7.909	1.417	12.68	1.443	14.75
7	1.023	1.075	5.129	1.188	16.16	1.092	6.746	1.124	9.905	1.174	14.77
8	0.7367	0.7586	2.977	0.8559	15.17	0.7927	7.599	0.8021	8.879	0.8269	12.24
22	0.7085	0.7348	3.703	0.8223	16.06	0.8202	15.77	0.7455	5.221	0.8220	16.01
23	1.009	1.044	3.380	1.128	11.76	1.187	17.56	1.068	5.796	1.114	10.34
25	1.257	1.314	4.500	1.427	13.47	1.490	18.53	1.332	5.916	1.393	10.79
27	1.023	1.054	3.084	1.172	14.57	1.185	15.89	1.096	7.151	1.118	9.372
28	0.7367	0.7605	3.228	0.8364	13.53	0.8448	14.67	0.7886	7.042	0.8101	9.962

NOTE (a): For Identification of the Designated Members and Nodes, See the Bridge Model Shown in Figure 2 of Appendix A.

Table 7. Impact Percentages - A Comparison Between Analytical Results, Test Values and A.R.E.A. - Specified Limits.

MEMBER[(a)]	MAXIMUM ANALYTICAL IMPACT -PERCENT	TOTAL A.R.E.A. SPECIFICATION IMPACT -PERCENT	MAXIMUM TEST (RECORDED) IMPACT -PERCENT
PRIEST RIVER BRIDGE (BRIDGE NO. 3 OF ANALYSIS)			
BOTTOM CHORD	12.14	24.7	13.8
TOP CHORD	9.47	24.7	5.4
HANGERS	24.59	44.0	14.9
DIAGONALS	20.25	24.7	6.2
END POSTS	12.0	24.7	11.5
DEVIL'S RIVER BRIDGE (BRIDGE NO. 4 OF ANALYSIS)			
BOTTOM CHORD	18.35	22.8	16.8
TOP CHORD	16.9	22.8	9.0
HANGERS	29.87	42.8	33.2
DIAGONALS	18.55	22.8	8.9
END POSTS	17.67	22.8	10.1

NOTE (a): For Identification of the Designated Members, See the Bridge Models Shown in Figures 1 and 2 of Appendix A.

8.4 Appendix D

Plots of Analytical Impact Percentages vs. Speed, for Bridge Member Stresses and Nodal Deflections in the Great Northern and Southern Pacific Bridges

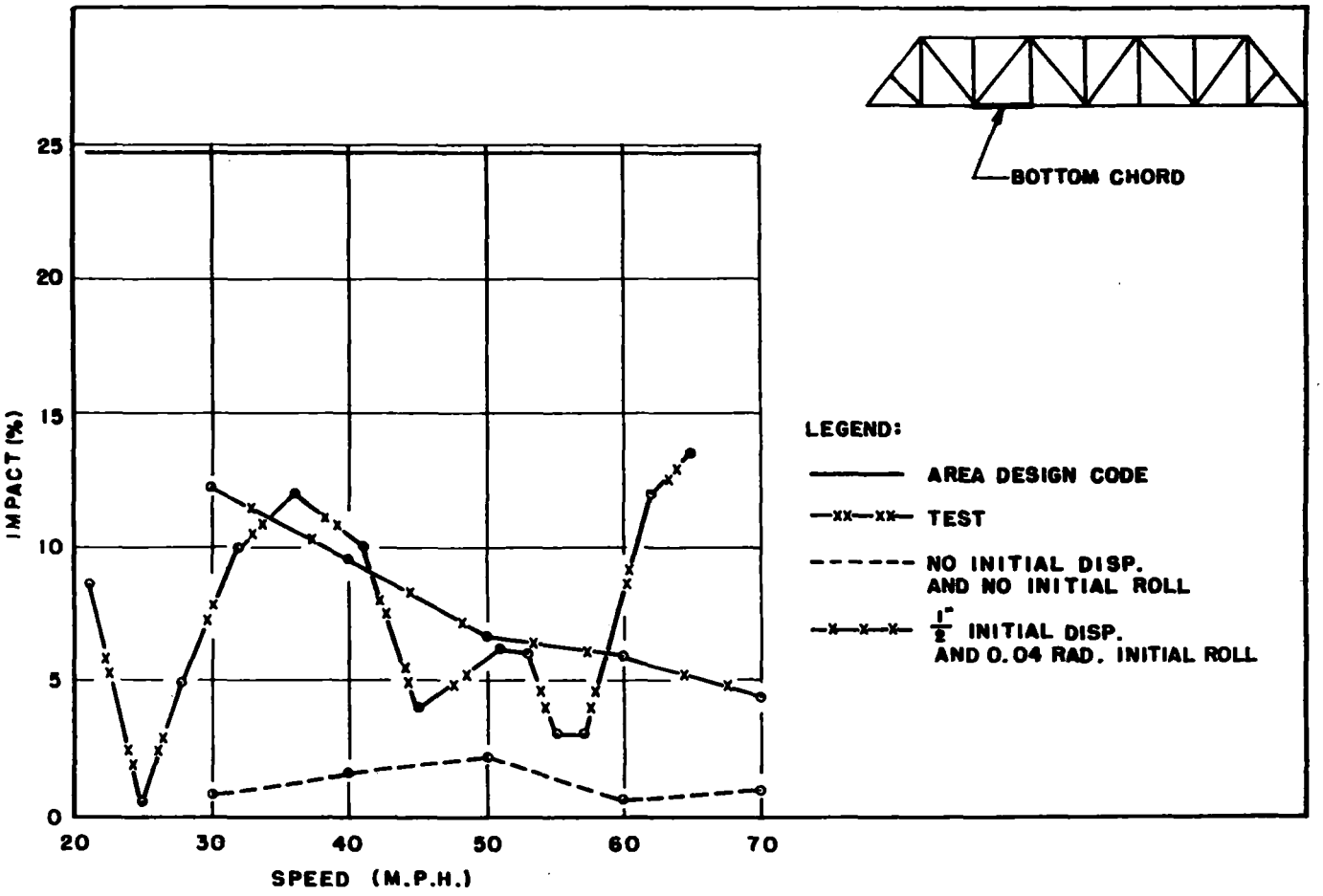

Figure 6.

Impact Values in a Bottom Chord, for a Train of Four-Axle Vehicles (Locomotive Suspension Stiffness of 7,000 Lbs./In., per Wheel; Car Suspension Stiffness of 11,200 Lbs./In., per Wheel) on the Priest River Bridge (Great Northern).

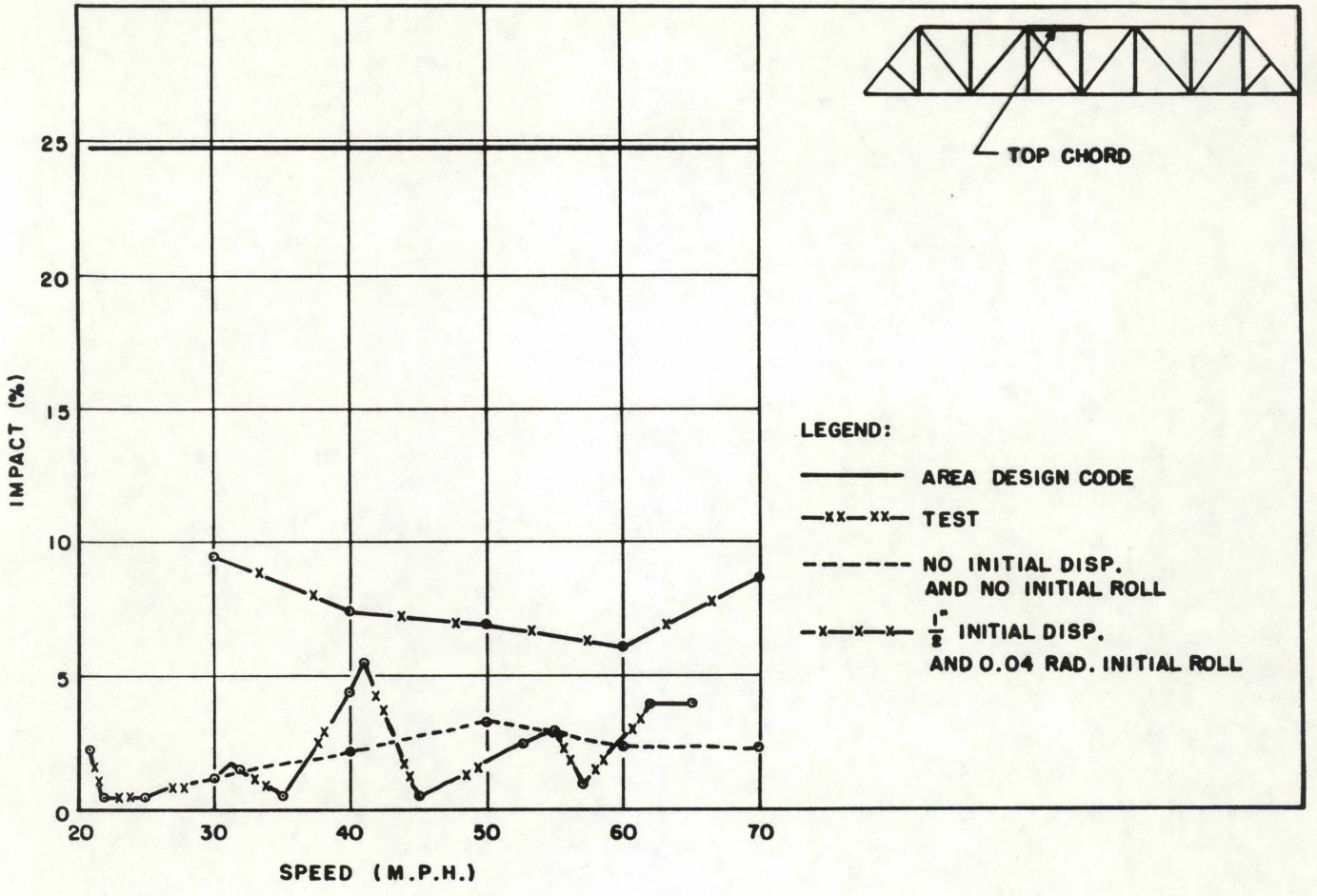

Figure 7.

Impact Values in a Top Chord, for a Train of Four-Axle Vehicles (Locomotive Suspension Stiffness of 7,000 Lbs./In., per Wheel; Car Suspension Stiffness of 11,200 Lbs./In., per Wheel) on the Priest River Bridge (Great Northern).

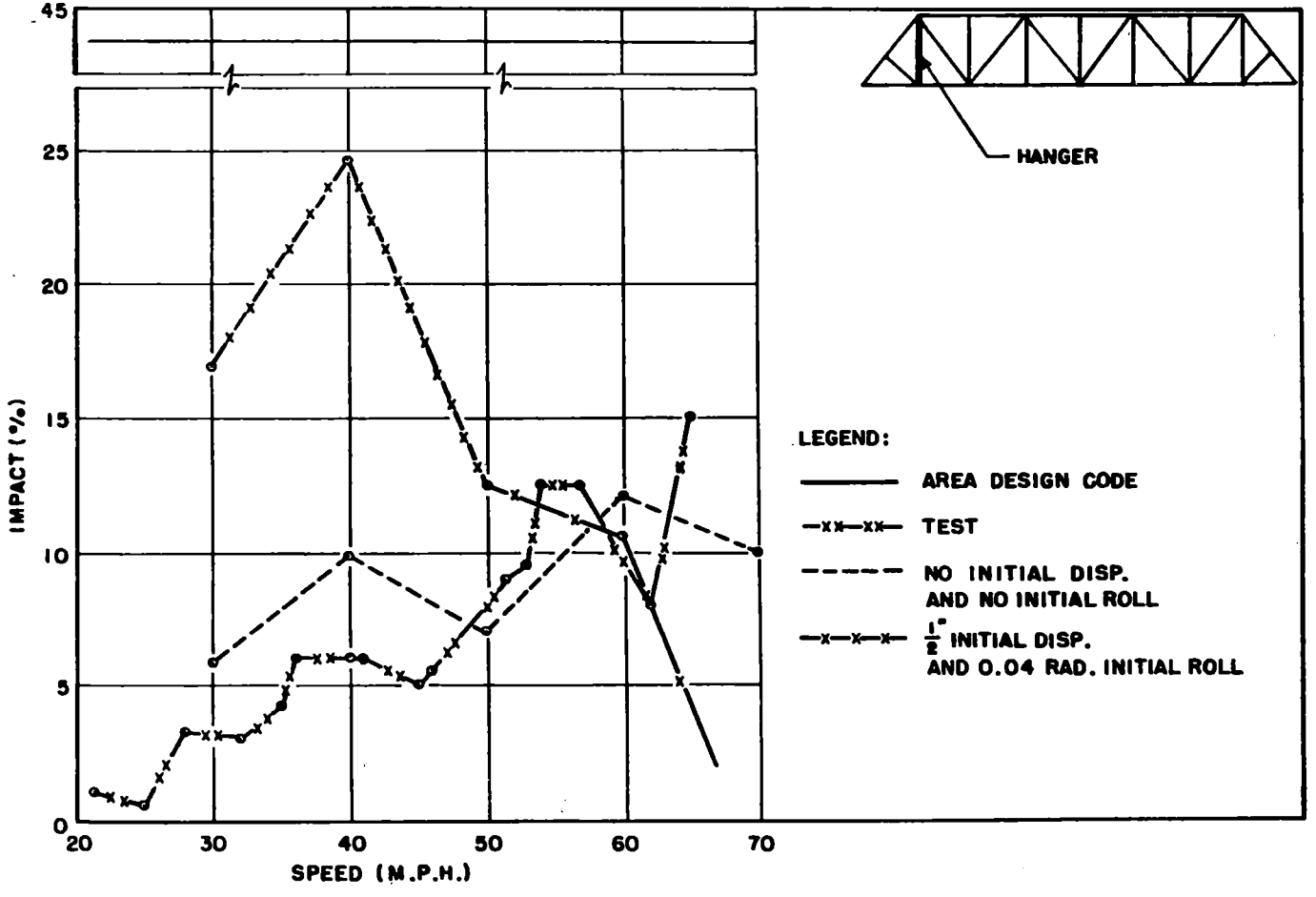

Figure 8.

Impact Values in a Hanger, for a Train of Four-Axle Vehicles (Locomotive Suspension Stiffness of 7,000 Lbs./In., per Wheel; Car Suspension Stiffness of 11,200 Lbs./In., per Wheel) on the Priest River Bridge (Great Northern).

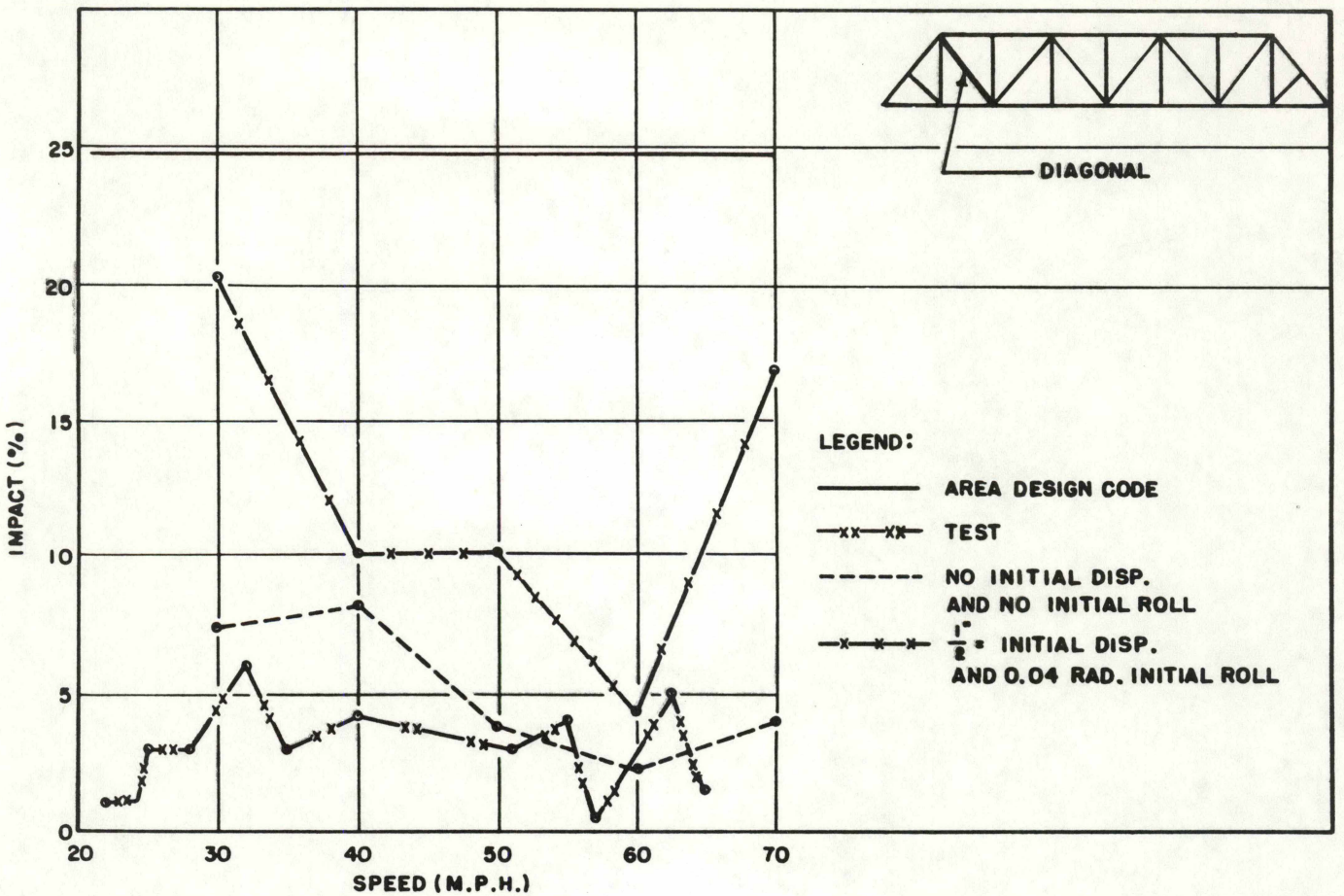

Figure 9.

Impact Values in a Diagonal, for a Train of Four-Axle Vehicles (Locomotive Suspension Stiffness of 7,000 Lbs./In., per Wheel; Car Suspension Stiffness of 11,200 Lbs./In., per Wheel) on the Priest River Bridge (Great Northern).

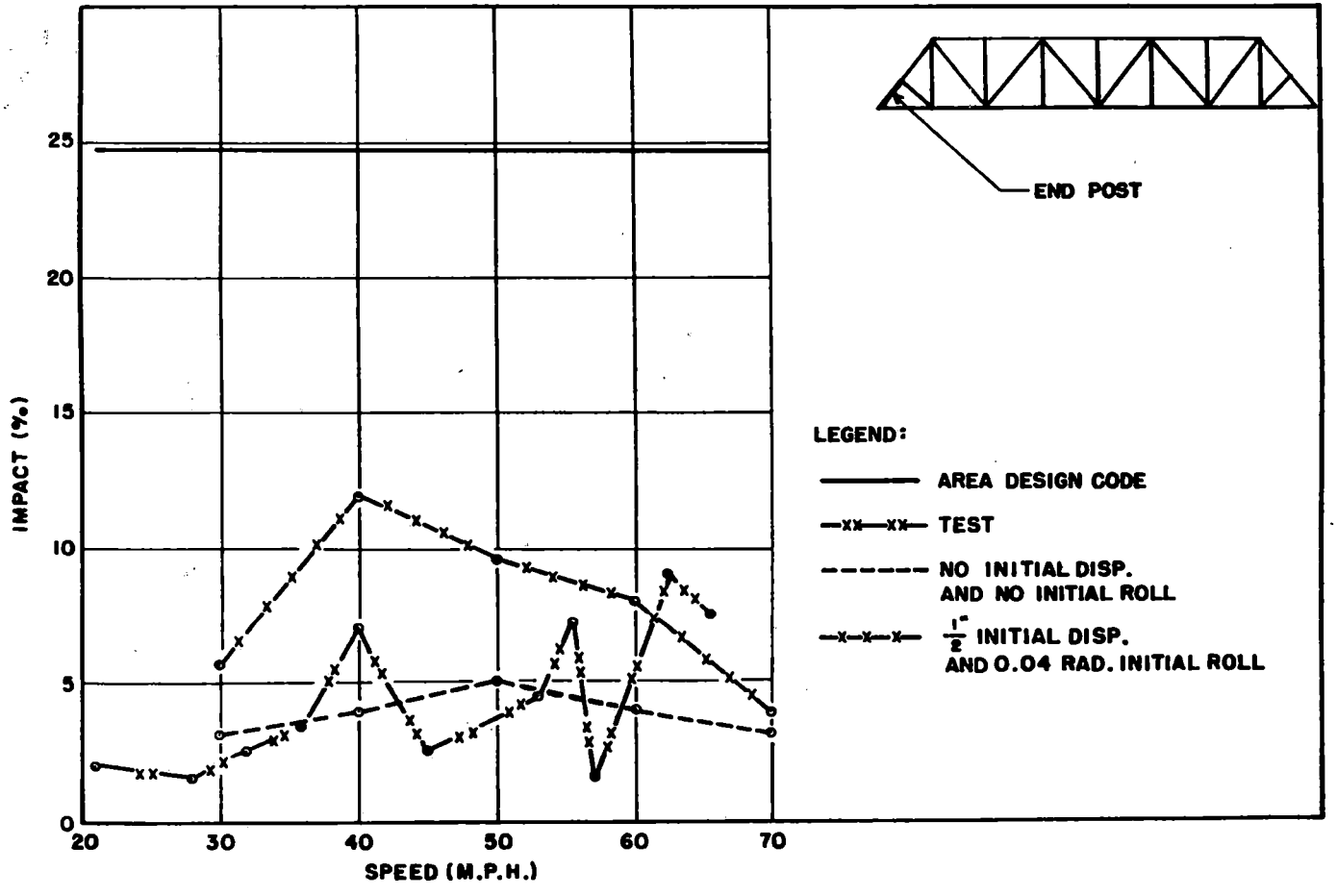

Figure 10.

Impact Values in an End Post, for a Train of Four-Axle Vehicles (Locomotive Suspension Stiffness of 7,000 Lbs./In., per Wheel; Car Suspension Stiffness of 11,200 Lbs./In., per Wheel) on the Priest River Bridge (Great Northern).

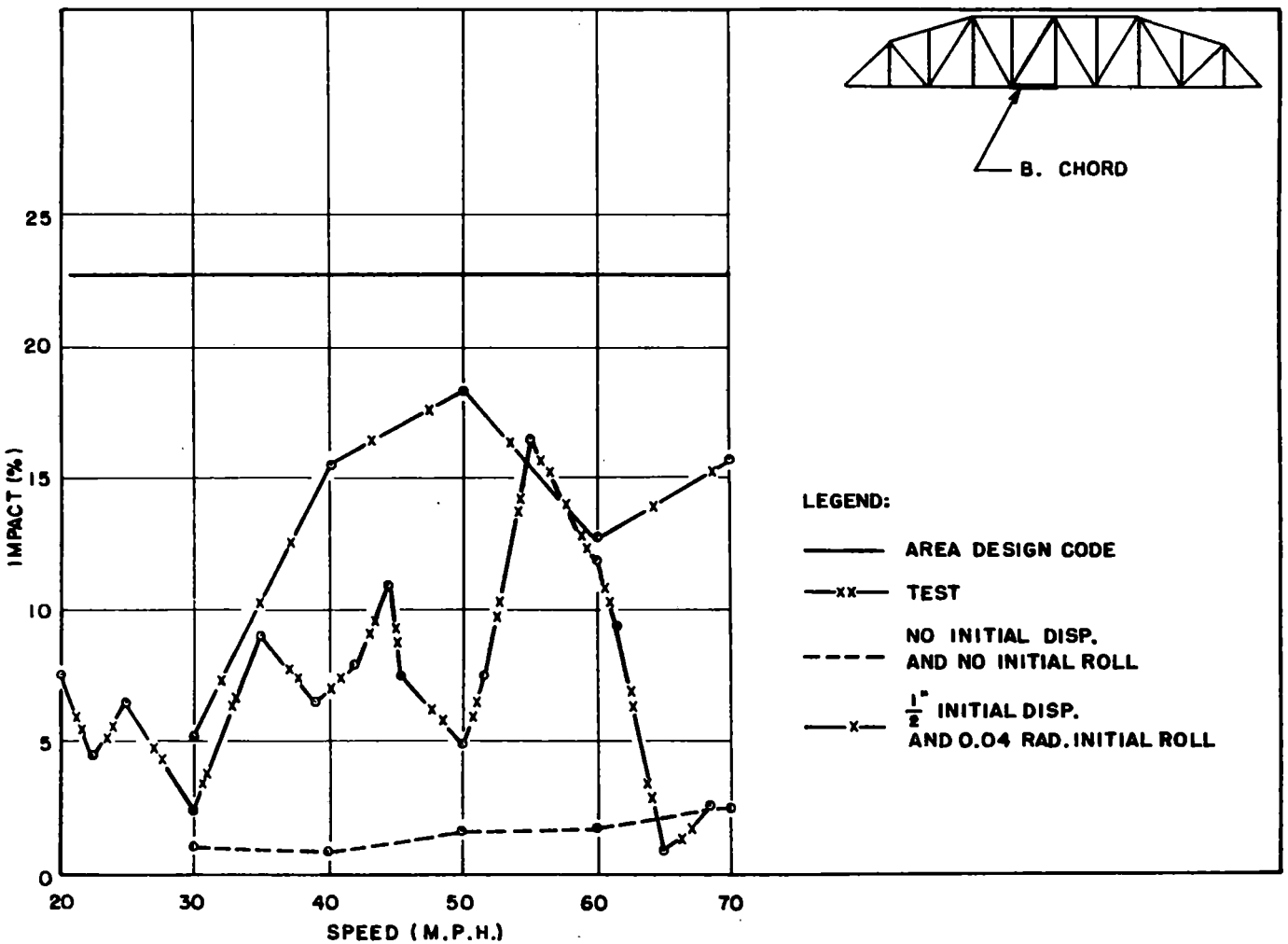

Figure 11.

Impact Values in a Bottom Chord, for a Train of Four-Axle Vehicles (Locomotive Suspension Stiffness of 7,000 Lbs./In., per Wheel; Car Suspension Stiffness of 11,200 Lbs./In., per Wheel) on the Devil's River Bridge (Southern Pacific).

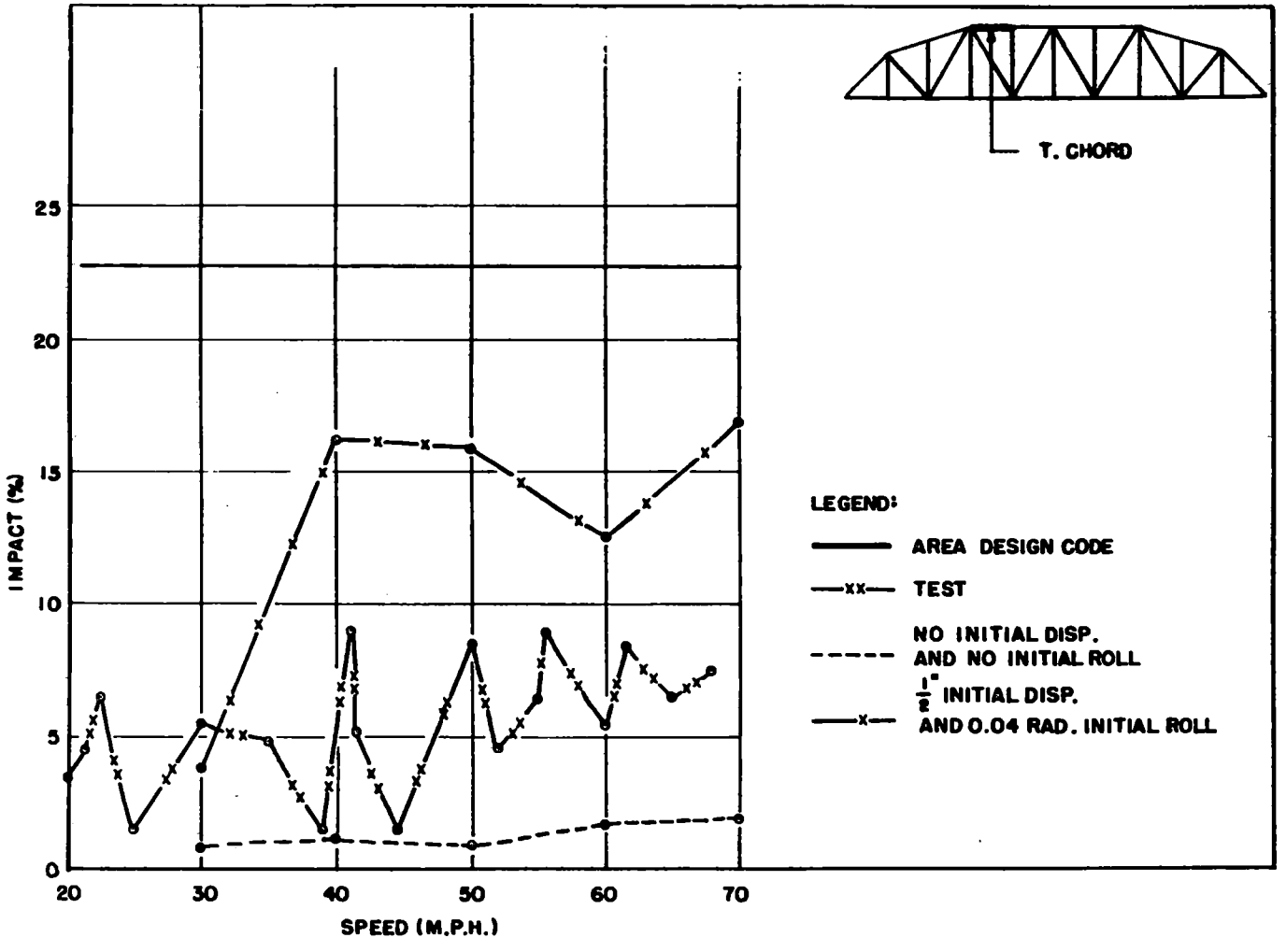

Figure 12.

Impact Values in a Top Chord, for a Train of Four-Axle Vehicles (Locomotive Suspension Stiffness of 7,000 Lbs./In., per Wheel; Car Suspension Stiffness of 11,200 Lbs./In., per Wheel) on the Devil's River Bridge (Southern Pacific).

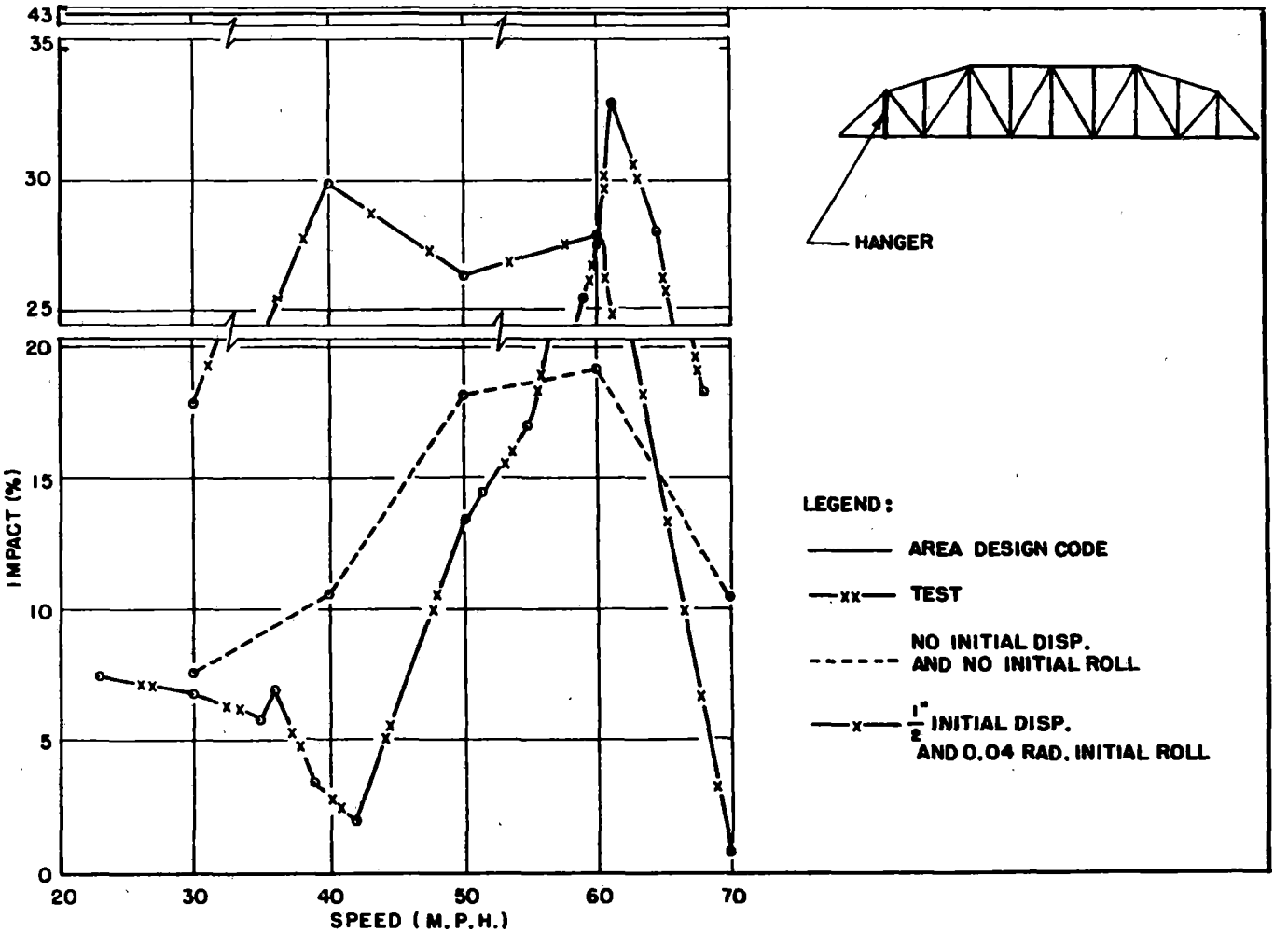

Figure 13.

Impact Values in a Hanger, for a Train of Four-Axle Vehicles (Locomotive Suspension Stiffness of 7,000 Lbs./In., per Wheel; Car Suspension Stiffness of 11,200 Lbs./In., per Wheel) on the Devil's River Bridge (Southern Pacific).

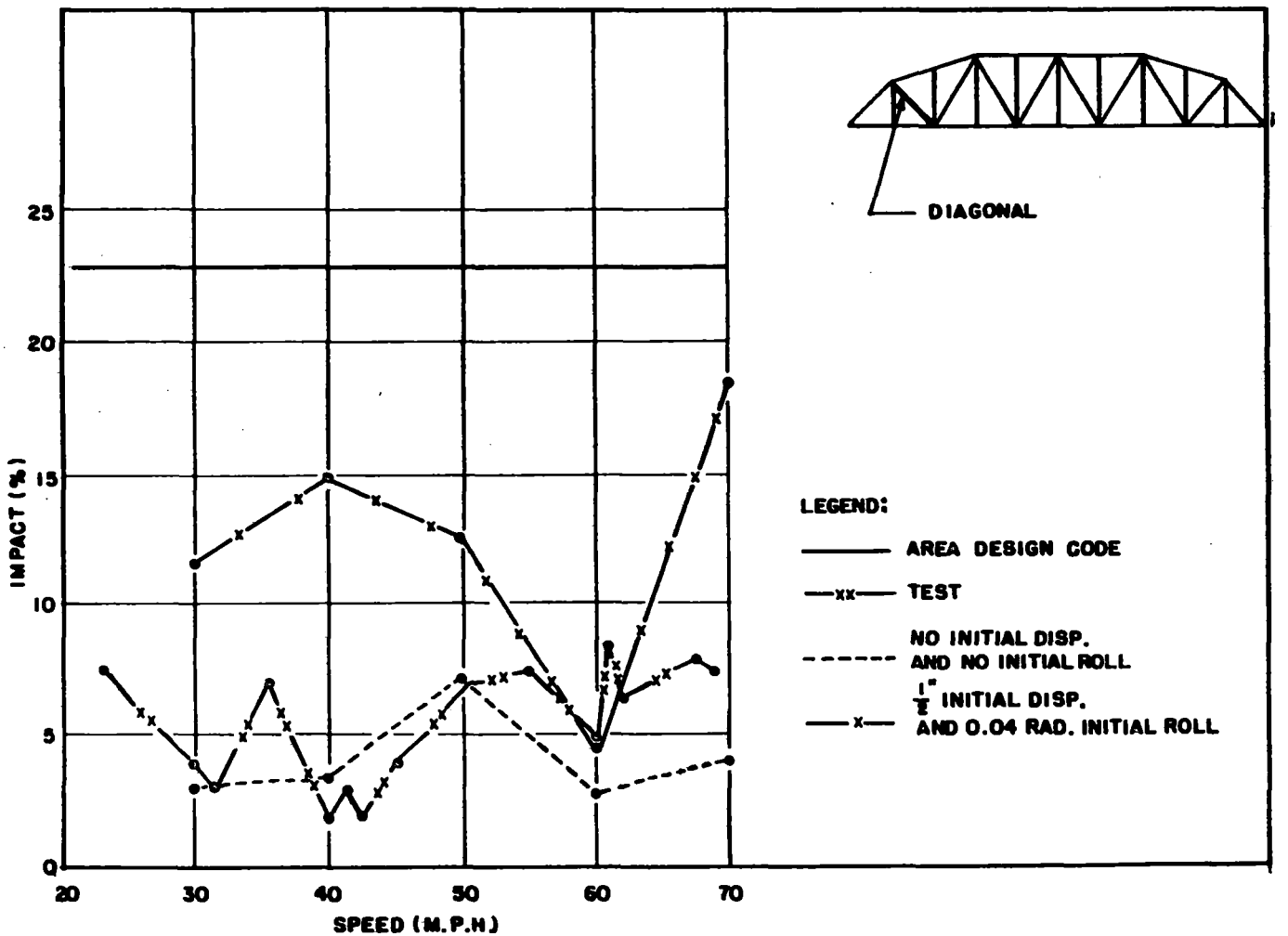

Figure 14.

Impact Values in a Diagonal, for a Train of Four-Axle Vehicles (Locomotive Suspension Stiffness of 7,000 Lbs./In., per Wheel; Car Suspension Stiffness of 11,200 Lbs./In., per Wheel) on the Devil's River Bridge (Southern Pacific).

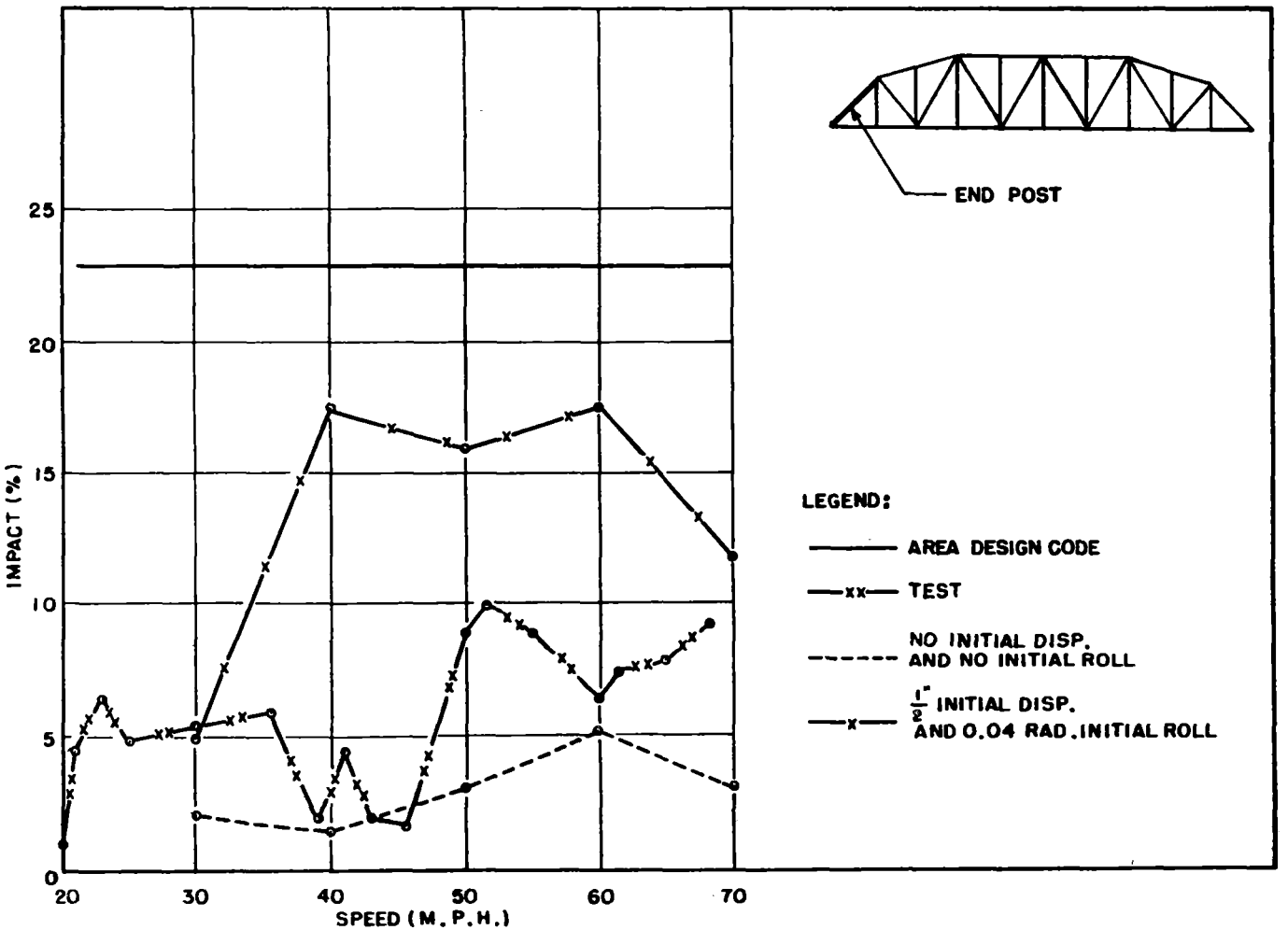

Figure 15.

Impact Values in an End Post, for a Train of Four-Axle Vehicles (Locomotive Suspension Stiffness of 7,000 Lbs./In., per Wheel; Car Suspension Stiffness of 11,200 Lbs./In., per Wheel) on the Devil's River Bridge (Southern Pacific).

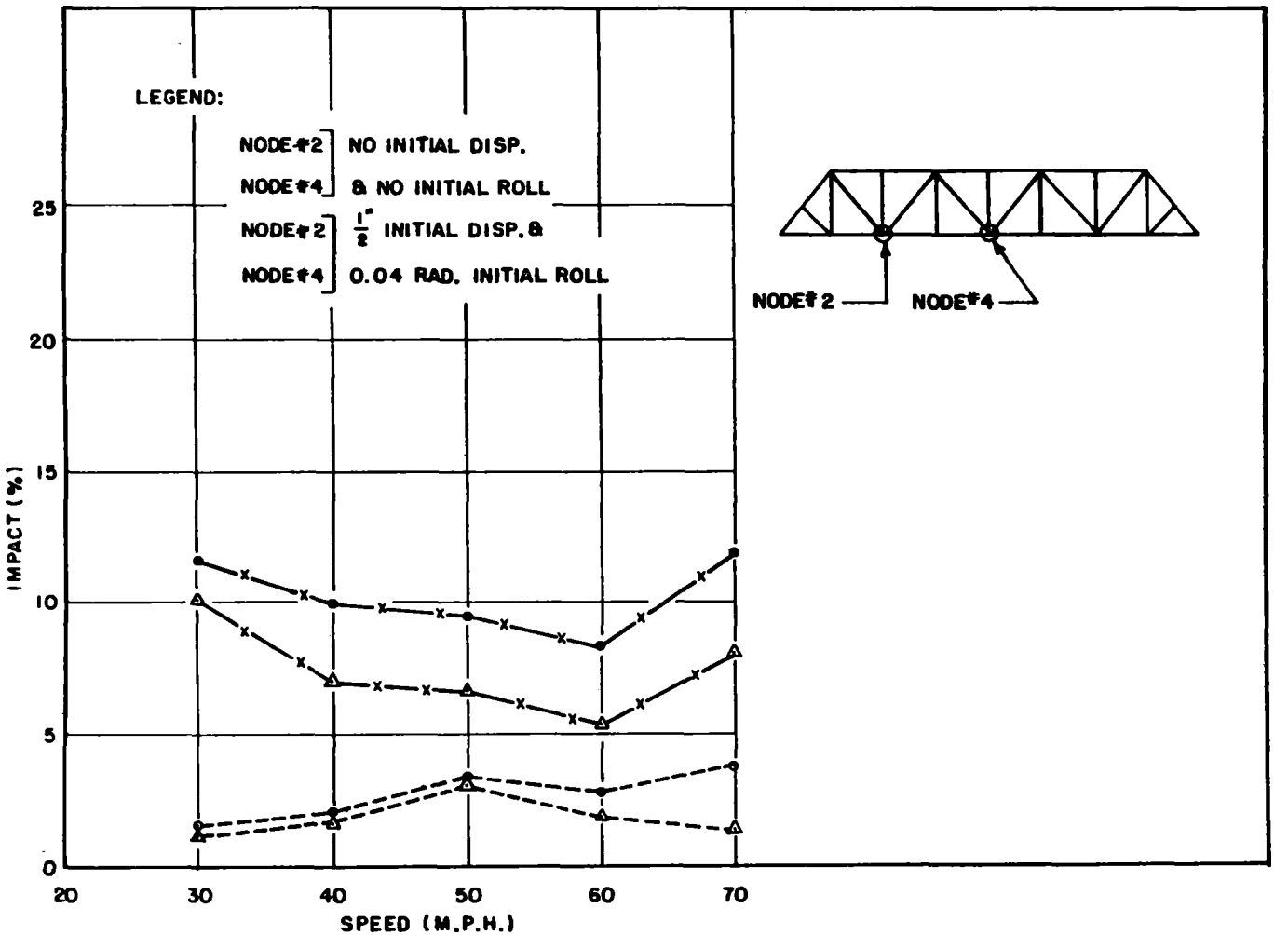

Figure 16.

Impact Values for the Designated Nodal Deflections for a Train of Four-Axle Vehicles (Locomotive Suspension Stiffness of 7,000 Lbs./In., per Wheel; Car Suspension Stiffness of 11,200 Lbs./In., per Wheel) on the Priest River Bridge (Great Northern).

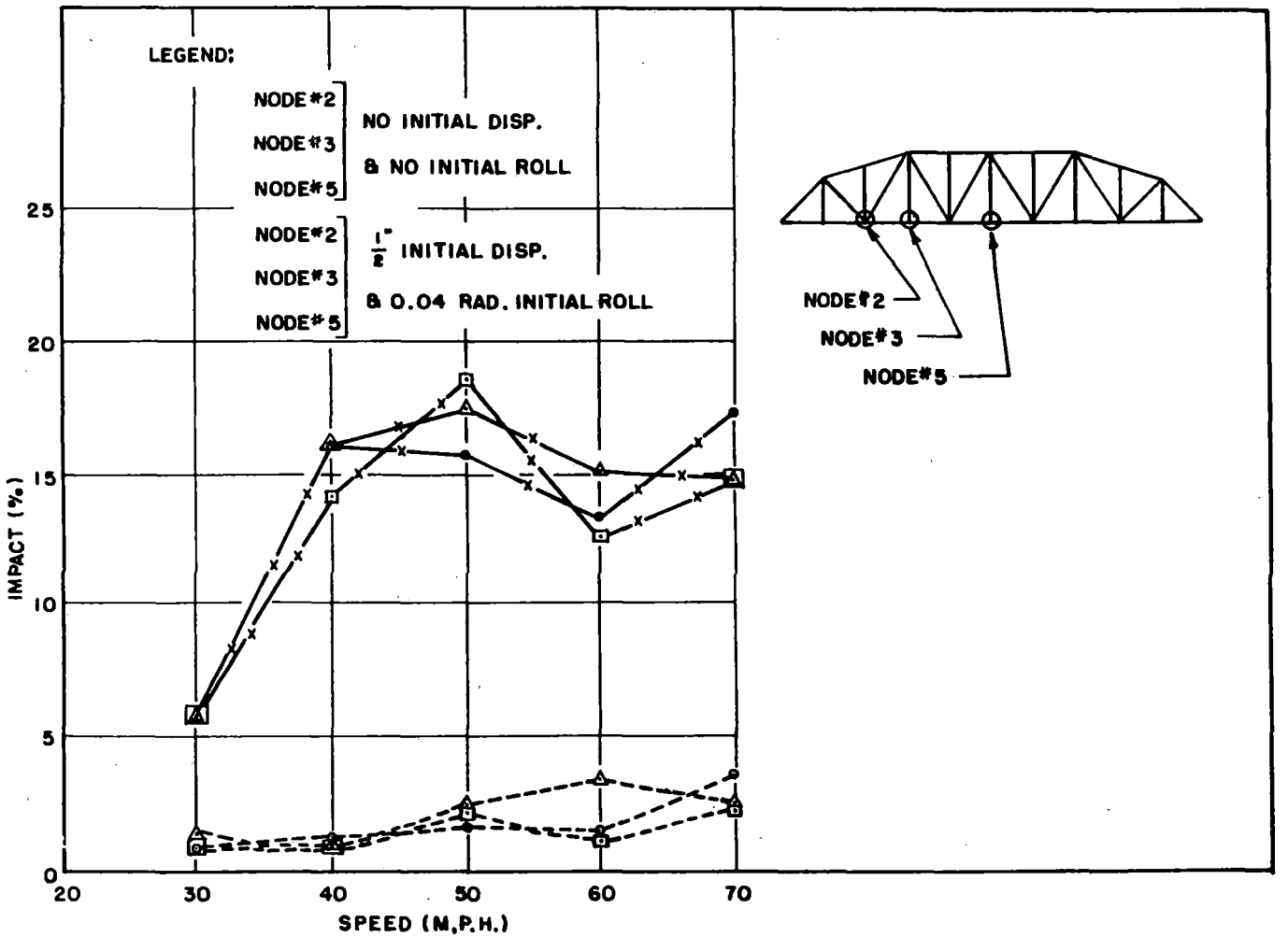

Figure 17.

Impact Values for the Designated Nodal Deflections for a Train of Four-Axle Vehicles (Locomotive Suspension Stiffness of 7,000 Lbs./In., per Wheel; Car Suspension Stiffness of 11,200 Lbs./In., per Wheel) on the Devil's River Bridge (Southern Pacific).

Dynamic Analysis of a Vehicle/Bridge System for Calculation of Impact Loads, 1981

Satya P Singh, Som P Singh, VK Garg